A mixed virtual element method for the Brinkman problem*

Ernesto Cáceres† Gabriel N. Gatica‡ Filánder A. Sequeira§

Abstract

In this paper we introduce and analyze a mixed virtual element method (mixed-VEM) for the two-dimensional Brinkman model of porous media flow with non-homogeneous Dirichlet boundary conditions. More precisely, we employ a dual-mixed formulation in which the only unknown is given by the pseudostress, whereas the velocity and pressure are computed via postprocessing formulae. We first recall the corresponding variational formulation, and then summarize the main mixed-VEM ingredients that are required for our discrete analysis. In particular, in order to define a calculable discrete bilinear form, whose continuous version involves deviatoric tensors, we propose two well-known alternatives for the local projector onto a suitable polynomial subspace, which allows the explicit integration of these terms. Next, we show that the global discrete bilinear form satisfies the hypotheses required by the Lax-Milgram Lemma. In this way, we conclude the well-posedness of our mixed-VEM scheme and derive the associated *a priori* error estimates for the virtual solution as well as for the fully computable projection of it. Furthermore, we also introduce a second element-by-element postprocessing formula for the pseudostress, which yields an optimally convergent approximation of this unknown with respect to the broken $\mathbb{H}(\mathbf{div})$-norm. Finally, several numerical results illustrating the good performance of the method and confirming the theoretical rates of convergence are presented.

Key words: Brinkman model, mixed virtual element method, a priori error analysis, postprocessing techniques, high-order approximations

1 Introduction

The Brinkman system, which describes the flow of a viscous fluid in a highly porous medium, and can be considered as a parameter-dependent combination of both the Darcy and Stokes equations, has become a very relevant model of study for numerical analysts of boundary value problems in fluid mechanics during the last few years (see, e.g. [2], [3], [4], [20], [21], [24], [25], [31], and the references therein). In particular, one of the most significant features of this problem arises from its relationship with the evolutive Stokes equations when a time stepping method is applied to them. Having said the above, and since we are mainly interested in mixed variational formulations, we first mention that, up to our knowledge, just a few references have dealt with mixed finite elements or related

*This work was partially supported by CONICYT-Chile through BASAL project CMM, Universidad de Chile, project Anillo ACT1118 (ANANUM), and the Becas-CONICYT Programme for foreign students; and by Centro de Investigación en Ingeniería Matemática (CI^{2}MA), Universidad de Concepción.

†CI^{2}MA and Departamento de Ingeniería Matemática, Universidad de Concepción, Casilla 160-C, Concepción, Chile, email: ecaceresv@udec.cl. Present Address: Division of Applied Mathematics, Brown University, Providence, RI 02912, USA.

‡CI^{2}MA and Departamento de Ingeniería Matemática, Universidad de Concepción, Casilla 160-C, Concepción, Chile, email: ggatica@ci2ma.udec.cl.

§Escuela de Matemática, Universidad Nacional de Costa Rica, Campus Omar Dengo, Heredia, Costa Rica, email: filander.sequeira@una.cr.

methods for this problem (see [20], [26], [27], and [31]). In particular, a dual mixed framework and a $\mathbf{H}(\mathrm{div})$-conforming finite elements combined with the symmetric interior penalty Galerkin method is employed in [26] to obtain a stable discrete formulation with respect to a mesh-dependent norm. The corresponding numerical study of the method proposed in [26] is performed in [27], in which, besides verifying the theoretical error estimates, the analysis is extended to the case of a non-constant permeability. In turn, a mixed formulation in which the flow vorticity is considered as an additional unknown is introduced in [31]. This approach differs from other vorticity-based formulations since it uses the de Rham sequence to derive an equation for this unknown, instead of obtaining it by taking the curl of the momentum equation.

Nevertheless, we also remark that no stress-based or pseudostress-based methods seemed to be available until the recent contribution [20]. Indeed, a new dual-mixed approach for the two-dimensional Brinkman equations, which includes an alternative way of dealing with mixed boundary conditions and the corresponding *a priori* and *a posteriori* error analyses, was introduced and analyzed there. More precisely, the pseudostress $\boldsymbol{\sigma}$ is the main unknown of the resulting saddle point problem in [20], whereas the velocity and pressure of the fluid are easily recovered in terms of $\boldsymbol{\sigma}$ through simple postprocessing formulae. In addition, as it is usual for this kind of methods, the Dirichlet boundary condition for the velocity becomes natural in this case, and the Neumann boundary condition, being essential, is imposed weakly through the introduction of the trace of the velocity on that boundary as the associated Lagrange multiplier. In this way, the Babuška-Brezzi theory is applied first in [20] to establish sufficient conditions for the well-posedness of the resulting continuous and discrete formulations. As a consequence, Raviart-Thomas elements of order $k \geq 0$ for the pseudostress, and continuous piecewise polynomials of degree $k+1$ for the Lagrange multiplier, become a feasible choice of finite element subspaces. Next, a reliable and efficient residual-based *a posteriori* error estimator is derived there. Suitable auxiliary problems, the continuous inf-sup conditions satisfied by the bilinear forms involved, a discrete Helmholtz decomposition, and the local approximation properties of the Raviart-Thomas and Clément interpolation operators are the main tools for proving the reliability. In turn, Helmholtz's decomposition, inverse inequalities, and the classical localization technique based on triangle-bubble and edge-bubble functions are employed to show the efficiency. Lately, a natural extension of the analysis and results from [20] to a class of Brinkman models whose viscosity depends nonlinearly on the gradient of the velocity, which is a characteristic feature of quasi-Newtonian Stokes flows, was developed in [21]. A reliable and efficient residual-based *a posteriori* error estimator was also derived in [21] by following basically the same approach from [20].

On the other hand, the virtual element method (VEM), introduced in [6] for the Poisson problem as a model, is one of the high-order discretization schemes that arised as a natural consequence of new developments and interpretations of the mimetic finite difference method (MFDM) (see, e.g. [12]). The main advantages of VEM approaches include an extension of the classical finite element technique to general polygonal and polyhedral meshes, and also as a generalization of the MFDM to arbitrary degrees of accuracy and arbitrary continuity properties. Additionally, as remarked in [8], other benefits of VEM, when compared with finite volume methods, MMFD, and related techniques, are given by its solid mathematical ground, the simplicity of the respective computational coding, and the quality of the numerical results provided. While most of the projectors employed originally to define the virtual element schemes were ad-hoc to the problem under consideration, it is interesting to highlight that the first attempts to derive a systematic use of the simple L^2-projection operator were introduced in [1], and then in [11] for the case of non-coercive bilinear forms. Furthermore, in the context of purely mixed virtual element techniques, that is based on dual-mixed variational formulations, the method was initially developed in [13], and more recently extended in [10], [9], and [17]. In particular, [10] corresponds to the extension of [1] to mixed formulations, whereas [9] generalizes the results of [10] to the case of variable coefficients. In turn, [17] provides the first analysis of a virtual element method for a mixed variational formulation of the Stokes problem in which the pseudostress and the

velocity are the only unknowns, whereas the pressure is computed via a postprocessing formula (see also [16] for further details). Therein, a new local projector onto a suitable space of polynomials is presented, which takes into account the main features of the continuous solution and allows the explicit integration of the terms involving the deviatoric tensors. The uniform boundedness of the resulting family of local projectors is established and its approximation properties are also derived. For several other contributions on VEM and mixed-VEM we refer for instance to [5], [7], [15], [19], and [29].

According to the above discussion, in the present paper we are interested in continuing the research line drawn by [20] and [17], and aim to develop a mixed-VEM approach for the two-dimensional Brinkman problem with non-homogeneous Dirichlet boundary conditions. To this end, we first proceed as in [20] and use both the equilibrium equation and the incompressibility condition to eliminate the velocity and pressure, respectively, so that the pseudostress becomes now the only unknown. Moreover, in order to define an explicitly computable bilinear form, we take advantage of the particular local projection defined in [17] as well as of the $\mathbb{L}^2$-orthogonal projection introduced and analyzed in [10] (see also [9]). In other words, we propose two mixed virtual element methods depending on two different projectors. The rest of this work is organized as follows. In Section 2 we introduce the boundary value problem of interest, and recall its pseudostress-based mixed formulation and the associated well-posedness result. Then, in Section 3 we follow [10] and [9] to introduce the virtual element subspace that will be employed. This includes the basic assumptions on the polygonal mesh, the definition of the local virtual element space, the projections and interpolants to be employed together with their respective approximation properties, and finally the definition itself of the global virtual element subspaces. Next, in Section 4 we introduce a fully calculable local discrete bilinear form, which depends on a suitable projection of the local virtual space, establish its boundedness and related properties, and describe two specific choices of that projection. In turn, in Section 5 we first set the corresponding mixed virtual element method, and apply the classical Lax-Milgram Lemma to deduce its well-posedness. Then, we employ suitable bounds and identities satisfied by the bilinear form and the projectors and interpolators involved, to derive the *a priori* error estimates and corresponding rates of convergence for the virtual solution as well as for the computable projection of it. In addition, we follow the ideas from [22] and [23] to construct a second approximation for the pseudostress variable $\boldsymbol{\sigma}$, which yields an optimal rate of convergence in the broken $\mathbb{H}(\mathbf{div})$-norm. Moreover, this new postprocessing formula can be used in general for any $\mathbf{H}(\mathrm{div})$-conforming VEM scheme. Finally, some numerical examples showing the good performance of the method, confirming the rates of convergence for regular and singular solutions, and illustrating the accurateness obtained with the approximate solutions, are reported in Section 6.

Notations

We end the present section by providing some notations to be used along the paper, including those already employed above. Indeed, given a bounded domain $\Omega \subseteq \mathrm{R}^2$ with boundary Γ, we let $\boldsymbol{n}$ be the outward unit normal vector on Γ. In addition, standard terminology will be adopted for Lebesgue spaces $\mathrm{L}^p(\Omega)$, $p > 1$, and Sobolev spaces $\mathrm{H}^s(\Omega)$, $s \in \mathrm{R}$, with norm $\|\cdot\|_{s,\Omega}$ and seminorm $|\cdot|_{s,\Omega}$. In particular, $\mathrm{H}^{1/2}(\Gamma)$ is the space of traces of functions of $\mathrm{H}^1(\Omega)$, and $\mathrm{H}^{-1/2}(\Gamma)$ denotes its dual. By $\mathbf{M}$ and $\mathbb{M}$ we will denote the corresponding vectorial and tensorial counterparts of the generic scalar functional space M. Then, letting $\mathbf{div}$ (resp. $\mathbf{rot}$) be the usual divergence operator div (resp. rotational operator rot) acting along the rows of a given tensor, we recall that the spaces

$$\mathbf{H}(\mathrm{div};\Omega) := \left\{\tau \in \mathbf{L}^2(\Omega) : \quad \mathrm{div}(\tau) \in \mathrm{L}^2(\Omega)\right\},$$

$$\mathbb{H}(\mathbf{div};\Omega) := \left\{\boldsymbol{\tau} \in \mathbb{L}^2(\Omega) : \quad \mathbf{div}(\boldsymbol{\tau}) \in \mathbf{L}^2(\Omega)\right\},$$

$$\mathbf{H}(\mathrm{rot};\Omega) := \left\{\tau \in \mathbf{L}^2(\Omega) : \quad \mathrm{rot}(\tau) \in \mathrm{L}^2(\Omega)\right\}$$

and

$$\mathbb{H}(\mathbf{rot};\Omega) := \Big\{ \boldsymbol{\tau} \in \mathbb{L}^2(\Omega) : \quad \mathbf{rot}(\boldsymbol{\tau}) \in \mathbf{L}^2(\Omega) \Big\},$$

equipped with the usual norms

$$\begin{aligned}
\|\tau\|^2_{\mathrm{div};\Omega} &:= \|\tau\|^2_{0,\Omega} + \|\mathrm{div}(\tau)\|^2_{0,\Omega} \qquad \forall\, \tau \in \mathbf{H}(\mathrm{div};\Omega)\,, \\
\|\boldsymbol{\tau}\|^2_{\mathbf{div};\Omega} &:= \|\boldsymbol{\tau}\|^2_{0,\Omega} + \|\mathbf{div}(\boldsymbol{\tau})\|^2_{0,\Omega} \qquad \forall\, \boldsymbol{\tau} \in \mathbb{H}(\mathbf{div};\Omega)\,, \\
\|\tau\|^2_{\mathrm{rot};\Omega} &:= \|\tau\|^2_{0,\Omega} + \|\mathrm{rot}(\tau)\|^2_{0,\Omega} \qquad \forall\, \tau \in \mathbf{H}(\mathrm{rot};\Omega)
\end{aligned}$$

and

$$\|\boldsymbol{\tau}\|^2_{\mathbf{rot};\Omega} := \|\boldsymbol{\tau}\|^2_{0,\Omega} + \|\mathbf{rot}(\boldsymbol{\tau})\|^2_{0,\Omega} \qquad \forall\, \boldsymbol{\tau} \in \mathbb{H}(\mathbf{rot};\Omega)\,,$$

are Hilbert spaces. Also, given $\boldsymbol{\tau} := (\tau_{ij})$, $\boldsymbol{\zeta} := (\zeta_{ij}) \in \mathrm{R}^{2\times 2}$, we write as usual

$$\boldsymbol{\tau}^{\mathtt{t}} := (\tau_{ji})\,, \quad \mathrm{tr}(\boldsymbol{\tau}) := \sum_{i=1}^{2} \tau_{ii}\,, \quad \boldsymbol{\tau}^{\mathrm{d}} := \boldsymbol{\tau} - \frac{1}{2}\,\mathrm{tr}(\boldsymbol{\tau})\,\mathbb{I}\,, \quad \text{and} \quad \boldsymbol{\tau} : \boldsymbol{\zeta} := \sum_{i,j=1}^{2} \tau_{ij}\zeta_{ij}\,,$$

where $\mathbb{I}$ is the identity matrix of $\mathbb{R} := \mathrm{R}^{2\times 2}$. Finally, in what follows we employ $\mathbf{0}$ to denote a generic null vector, null tensor or null operator, and use C, with or without subscripts, bars, tildes or hats, to denote generic constants independent of the discretization parameters, which may take different values at different places.

2 The Brinkman problem and its pseudostress-based formulation

Let Ω be a bounded and simply connected polygonal domain in R^2 with boundary Γ. Our goal is to determine the velocity $\mathbf{u}$, the pseudostress $\boldsymbol{\sigma}$, and the pressure p of a steady Brinkman flow occupying the region Ω. In other words, given a volume force $\mathbf{f} \in \mathbf{L}^2(\Omega)$ and a Dirichlet datum $\mathbf{g} \in \mathbf{H}^{1/2}(\Gamma)$, we seek a tensor field $\boldsymbol{\sigma}$, a vector field $\mathbf{u}$ and a scalar field p such that

$$\begin{aligned}
&\boldsymbol{\sigma} = \mu\,\nabla\mathbf{u} - p\,\mathbb{I} \quad \text{in } \Omega\,, \qquad \alpha\,\mathbf{u} - \mathbf{div}(\boldsymbol{\sigma}) = \mathbf{f} \quad \text{in } \Omega\,, \\
&\mathrm{div}(\mathbf{u}) = 0 \quad \text{in } \Omega\,, \qquad \mathbf{u} = \mathbf{g} \quad \text{on } \Gamma\,, \qquad \int_\Omega p = 0\,,
\end{aligned} \tag{2.1}$$

where μ is the dynamic viscosity, and $\alpha > 0$ is a constant approximation of the viscosity divided by the permeability. In addition, as required by the incompressibility condition, we assume from now on that the datum $\mathbf{g}$ satisfies the compatibility condition $\int_\Gamma \mathbf{g}\cdot\boldsymbol{n} = 0$. Furthermore, the incompressibility condition also implies that (2.1) can be rewritten as:

$$\frac{1}{\mu}\,\boldsymbol{\sigma}^{\mathrm{d}} = \nabla\mathbf{u} \quad \text{in } \Omega\,, \quad \alpha\,\mathbf{u} - \mathbf{div}(\boldsymbol{\sigma}) = \mathbf{f} \quad \text{in } \Omega\,, \quad \mathbf{u} = \mathbf{g} \quad \text{on } \Gamma\,, \quad \int_\Omega \mathrm{tr}(\boldsymbol{\sigma}) = 0\,, \tag{2.2}$$

where the pressure p can be obtained by the postprocessing formula

$$p = -\frac{1}{2}\,\mathrm{tr}(\boldsymbol{\sigma}) \quad \text{in } \Omega\,. \tag{2.3}$$

Then, proceeding as in [20], the velocity is replaced from the second equation of (2.2), that is

$$\mathbf{u} = \frac{1}{\alpha}\big\{\mathbf{f} + \mathbf{div}(\boldsymbol{\sigma})\big\} \quad \text{in } \Omega\,, \tag{2.4}$$

which yields the following dual-mixed variational formulation of (2.2): Find $\boldsymbol{\sigma} \in \mathbb{H}$ such that

$$a(\boldsymbol{\sigma},\boldsymbol{\tau}) = F(\boldsymbol{\tau}) \qquad \forall\, \boldsymbol{\tau} \in \mathbb{H}\,, \tag{2.5}$$

where

$$\mathbb{H} := \mathbb{H}_0(\mathbf{div};\Omega) := \left\{ \boldsymbol{\tau} \in \mathbb{H}(\mathbf{div};\Omega) : \quad \int_\Omega \mathrm{tr}(\boldsymbol{\tau}) \,=\, 0 \right\},$$

$a : \mathbb{H} \times \mathbb{H} \to \mathrm{R}$ is the bilinear form

$$a(\boldsymbol{\zeta},\boldsymbol{\tau}) \;:=\; \frac{1}{\mu}\int_\Omega \boldsymbol{\zeta}^{\mathrm{d}} : \boldsymbol{\tau}^{\mathrm{d}} \;+\; \frac{1}{\alpha}\int_\Omega \mathbf{div}(\boldsymbol{\zeta})\cdot\mathbf{div}(\boldsymbol{\tau}) \qquad \forall\, \boldsymbol{\zeta},\, \boldsymbol{\tau} \,\in\, \mathbb{H},$$

and $F : \mathbb{H} \to \mathrm{R}$ is the linear functional

$$F(\boldsymbol{\tau}) \,:=\, -\frac{1}{\alpha}\int_\Omega \mathbf{f}\cdot\mathbf{div}(\boldsymbol{\tau}) \,+\, \langle \boldsymbol{\tau}\boldsymbol{n}, \mathbf{g}\rangle_\Gamma \qquad \forall\, \boldsymbol{\tau} \in \mathbb{H}.$$

In what follows we proceed as in [20] to derive the well-posedness of (2.5). We begin with the following technical result taken from [14].

Lemma 2.1. *There exists $c_\Omega > 0$, depending only on Ω, such that*

$$c_\Omega \,\|\boldsymbol{\tau}\|^2_{0,\Omega} \;\leq\; \|\boldsymbol{\tau}^{\mathrm{d}}\|^2_{0,\Omega} \;+\; \|\mathbf{div}(\boldsymbol{\tau})\|^2_{0,\Omega} \qquad \forall\, \boldsymbol{\tau} \in \mathbb{H}.$$

Proof. See [14, Chapter IV, Proposition 3.1]. □

Then the $\mathbb{H}$-ellipticity of a is proved as follows.

Lemma 2.2. *There exists $\eta > 0$, depending only on μ, α and Ω, such that*

$$a(\boldsymbol{\zeta},\, \boldsymbol{\zeta}) \;\;\geq\;\; \eta\, \|\boldsymbol{\zeta}\|^2_{\mathbf{div};\Omega} \qquad \forall\, \boldsymbol{\zeta} \in \mathbb{H}.$$

Proof. According to the definition of a and Lemma 2.1, we find that for each $\boldsymbol{\zeta} \in \mathbb{H}$ there holds

$$a(\boldsymbol{\zeta},\boldsymbol{\zeta}) \,=\, \frac{1}{\mu}\,\|\boldsymbol{\zeta}^{\mathrm{d}}\|^2_{0,\Omega} \,+\, \frac{1}{\alpha}\,\|\mathbf{div}(\boldsymbol{\zeta})\|^2_{0,\Omega} \,\geq\, \eta\,\|\boldsymbol{\zeta}\|^2_{\mathbf{div};\Omega},$$

where $\eta := \min\{c_\Omega\eta_0, \frac{1}{2\alpha}\}$ and $\eta_0 := \min\{\frac{1}{\mu}, \frac{1}{2\alpha}\}$. □

The unique solvability of (2.5) is established next.

Theorem 2.1. *Assume that $\mathbf{f} \in \mathbf{L}^2(\Omega)$ and $\mathbf{g} \in \mathbf{H}^{1/2}(\Gamma)$. Then, there exists a unique solution $\boldsymbol{\sigma} \in \mathbb{H}$ to* (2.5)*. In addition, there exists $C > 0$ such that*

$$\|\boldsymbol{\sigma}\|_{\mathbf{div};\Omega} \,\leq\, C\left\{\|\mathbf{f}\|_{0,\Omega} \;+\; \|\mathbf{g}\|_{1/2,\Gamma}\right\}.$$

Proof. Thanks to the ellipticity of a and the boundedness of F, the proof is a straightforward application of the Lax-Milgram Lemma. □

3 The virtual element subspace

The main purpose of this section is to introduce a virtual element subspace $\mathbb{H}_h$ of $\mathbb{H} := \mathbb{H}_0(\mathbf{div};\Omega)$, with which we prove later on that the mixed virtual element scheme associated with the continuous formulation (2.5) is well-posed. To this end, we follow the approach from [10, 9] to define first a virtual element subspace of $\mathbf{H}(\mathrm{div};\Omega)$, and then proceed row-wise to extend the above to $\mathbb{H}(\mathbf{div};\Omega)$. Along the way, local virtual element spaces, suitable associated interpolation operators, and their main approximation properties are also provided. While all these results are available in [10] and [9], for convenience of the reader we recall here most of the corresponding details.

3.1 Basic assumptions

We begin by letting $\{\mathcal{T}_h\}_{h>0}$ be a family of decompositions of Ω in polygonal elements. Then, for each $K \in \mathcal{T}_h$ we let d_K be the number of its edges and denote its diameter by h_K. In addition, we define as usual $h := \max\{h_K : K \in \mathcal{T}_h\}$. Furthermore, in what follows we assume that there exists a constant $C_{\mathcal{T}} > 0$ such that for each decomposition $\mathcal{T}_h$ and for each $K \in \mathcal{T}_h$ there hold:

a) the ratio between the shortest edge and the diameter h_K of K is bigger than $C_{\mathcal{T}}$, and

b) K is star-shaped with respect to a ball B of radius $C_{\mathcal{T}} h_K$ and center $\mathbf{x}_B \in K$, that is, for each $\mathbf{x}_0 \in B$, all the line segments joining $\mathbf{x}_0$ with any $\mathbf{x} \in K$ are contained in K, or, equivalently, for each $\mathbf{x} \in K$, the closed convex hull of $\{\mathbf{x}\} \cup B$ is contained in K.

As a consequence of the above hypotheses, one can show that each $K \in \mathcal{T}_h$ is simply connected, and that there exists an integer $N_{\mathcal{T}}$ (depending only on $C_{\mathcal{T}}$), such that for each $K \in \mathcal{T}_h$, d_K is bounded above by $N_{\mathcal{T}}$.

3.2 The local virtual element space

In what follows, given an integer $\ell \geq 0$ and $U \subseteq \mathrm{R}^2$, we let $\mathrm{P}_\ell(U)$ be the space of polynomials defined in U of total degree at most ℓ. Then, for each integer $k \geq 0$ and for each $K \in \mathcal{T}_h$, we introduce the local virtual element space of order k (see, e.g. [10, 9])

$$\begin{aligned}\mathbf{H}_k^K := \Big\{ \tau := (\tau_1, \tau_2)^{\mathtt{t}} \in \mathbf{H}(\mathrm{div}; K) \cap \mathbf{H}(\mathrm{rot}; K) : \quad \tau \cdot \boldsymbol{n}|_e \in \mathrm{P}_k(e) \quad \forall \text{ edge } e \in \partial K \,, \\ \mathrm{div}(\tau) \in \mathrm{P}_k(K) \,, \quad \text{and} \quad \mathrm{rot}(\tau) \in \mathrm{P}_{k-1}(K) \Big\} \,,\end{aligned} \tag{3.1}$$

where $\mathrm{rot}(\tau) := \frac{\partial \tau_2}{\partial x_1} - \frac{\partial \tau_1}{\partial x_2}$ and $\mathrm{P}_{-1}(K) := \{0\}$. In addition, given an edge $e \in \mathcal{T}_h$ with medium point x_e and length h_e, we consider the following set of $k+1$ normalized monomials on e:

$$\mathcal{B}_k(e) := \left\{ \left(\frac{x - x_e}{h_e} \right)^j \right\}_{0 \leq j \leq k} , \tag{3.2}$$

which certainly constitutes a basis of $\mathrm{P}_k(e)$. Similarly, given an integer $\ell \geq 0$ and an element $K \in \mathcal{T}_h$ with barycenter $\mathbf{x}_K$, we define the following set of $\frac{1}{2}(\ell+1)(\ell+2)$ normalized monomials

$$\mathcal{B}_\ell(K) := \left\{ \left(\frac{\mathbf{x} - \mathbf{x}_K}{h_K} \right)^{\boldsymbol{\alpha}} \right\}_{0 \leq |\boldsymbol{\alpha}| \leq \ell} , \tag{3.3}$$

which is a basis of $\mathrm{P}_\ell(K)$. We remark here that (3.3) makes use of the multi-index notation, where, given $\mathbf{x} := (x_1, x_2)^{\mathtt{t}} \in \mathrm{R}^2$ and $\boldsymbol{\alpha} := (\alpha_1, \alpha_2)^{\mathtt{t}}$, with nonnegative integers α_1, α_2, we set $\mathbf{x}^\alpha := x_1^{\alpha_1} x_2^{\alpha_2}$ and $|\boldsymbol{\alpha}| := \alpha_1 + \alpha_2$. Next, we recall from [10, 9] the following local degrees of freedom for a given $\tau \in \mathbf{H}_k^K$

$$\begin{aligned} m_{q,e}^{\boldsymbol{n}}(\tau) &:= \int_e \tau \cdot \boldsymbol{n}\, q \quad \forall\, q \in \mathcal{B}_k(e) \,, \quad \forall \text{ edge } e \in \partial K \,, \\ m_{q,K}^{\mathrm{div}}(\tau) &:= \int_K \tau \cdot \nabla q \quad \forall\, q \in \mathcal{B}_k(K) \setminus \{1\} \,, \\ m_{\mathbf{q},K}^{\mathrm{rot}}(\tau) &:= \int_K \tau \cdot \mathbf{q} \quad \forall\, \mathbf{q} \in \mathcal{G}_k(K) \,, \end{aligned} \tag{3.4}$$

where $\mathcal{G}_k(K)$ is a basis of $\big(\nabla \mathrm{P}_{k+1}(K)\big)^{\perp} \cap \mathbf{P}_k(K)$, which is the $\mathbf{L}^2(K)$-orthogonal of $\nabla \mathrm{P}_{k+1}(K)$ in $\mathbf{P}_k(K)$. Then, thanks to the cardinalities of $\mathcal{B}_k(e)$ and $\mathcal{B}_k(K)$, and according to the dimensions of $\mathbf{P}_k(K)$ and $\nabla \mathrm{P}_{k+1}(K)$ (see also [16, Lemma 4.3.1] for details on the latter), we find that the cardinality of $\mathcal{G}_k(K)$ is $\frac{k(k+1)}{2}$, and hence the amount of local degrees of freedom defined in (3.4) is given by

$$n_k^K \;:=\; (k+1)\,d_K \;+\; \left\{\frac{(k+1)(k+2)}{2} - 1\right\} \;+\; \frac{k(k+1)}{2} \;=\; (k+1)(d_K + k + 1) - 1\,.$$

Moreover, it is not difficult to prove that for each $K \in \mathcal{T}_h$ these n_k^K local degrees of freedom are unisolvent in $\mathbf{H}_k^K$ (see [10, Section 3.4]).

According to the above discussion, we are now able to define for each $K \in \mathcal{T}_h$ the tensorial local virtual element space

$$\mathbb{H}_k^K \;:=\; \Big\{\boldsymbol{\tau} \in \mathbb{H}(\mathbf{div}; K) \cap \mathbb{H}(\mathbf{rot} : K) : \quad (\tau_{i1},\, \tau_{i2})^{\mathtt{t}} \in \mathbf{H}_k^K \quad \forall\, i \in \{1,2\}\Big\}\,, \tag{3.5}$$

which is certainly unisolvent with respect to the $2n_k^K$ degrees of freedom

$$\begin{aligned}
\mathbf{m}^{\boldsymbol{n}}_{\mathbf{q},e}(\boldsymbol{\tau}) \;&:=\; \int_e \boldsymbol{\tau}\boldsymbol{n}\cdot\mathbf{q} \qquad \forall\, \mathbf{q} \in \boldsymbol{\mathcal{B}}_k(e)\,, \quad \forall \text{ edge } e \in \partial K\,,\\
\mathbf{m}^{\mathbf{div}}_{\mathbf{q},K}(\boldsymbol{\tau}) \;&:=\; \int_K \boldsymbol{\tau} : \nabla\mathbf{q} \quad \forall\, \mathbf{q} \in \boldsymbol{\mathcal{B}}_k(K) \setminus \{(1,0)^{\mathtt{t}},\, (0,1)^{\mathtt{t}}\}\,,\\
\mathbf{m}^{\mathbf{rot}}_{\boldsymbol{\rho},K}(\boldsymbol{\tau}) \;&:=\; \int_K \boldsymbol{\tau} : \boldsymbol{\rho} \qquad \forall\, \boldsymbol{\rho} \in \boldsymbol{\mathcal{G}}_k(K)\,,
\end{aligned} \tag{3.6}$$

where

$$\begin{aligned}
\boldsymbol{\mathcal{B}}_k(e) &:= \big\{(q,0)^{\mathtt{t}} :\; q \in \mathcal{B}_k(e)\big\} \,\cup\, \big\{(0,q)^{\mathtt{t}} :\; q \in \mathcal{B}_k(e)\big\}\,,\\
\boldsymbol{\mathcal{B}}_k(K) &:= \big\{(q,0)^{\mathtt{t}} :\; q \in \mathcal{B}_k(K)\big\} \,\cup\, \big\{(0,q)^{\mathtt{t}} :\; q \in \mathcal{B}_k(K)\big\}\,,
\end{aligned}$$

and

$$\boldsymbol{\mathcal{G}}_k(K) := \left\{\begin{pmatrix} \mathbf{q} \\ \mathbf{0} \end{pmatrix} :\; \mathbf{q} \in \mathcal{G}_k(K)\right\} \cup \left\{\begin{pmatrix} \mathbf{0} \\ \mathbf{q} \end{pmatrix} :\; \mathbf{q} \in \mathcal{G}_k(K)\right\}.$$

For sake of completeness, we now describe the explicit computation of the basis $\mathcal{G}_k(K)$. In fact, given $K \in \mathcal{T}_h$, we first denote by $\{\varphi_i^K\}_{i=1}^{m_k}$ the elements of $\mathcal{B}_{k+1}(K)$ ($m_k := \frac{1}{2}(k+2)(k+3)$), which certainly constitute a hierarchical basis of $\mathrm{P}_{k+1}(K)$, and let $\{\boldsymbol{\psi}_j^K\}_{j=1}^{2d_k}$ be the basis of $\mathbf{P}_k(K)$ given by

$$\boldsymbol{\psi}_j^K \;:=\; \begin{cases} (\varphi_j^K, 0)^{\mathtt{t}} & \text{if } \; 1 \le j \le d_k\,, \\ (0, \varphi_{j-d_k}^K)^{\mathtt{t}} & \text{otherwise}\,, \end{cases} \qquad \forall\, j \in \{1,\ldots,2d_k\}\,,$$

where $d_k := \frac{1}{2}(k+1)(k+2)$. Hence, setting $\mathcal{G}_k(K) := \{\mathbf{q}_\ell^K\}_{\ell=1}^{r_k}$, with $r_k := \frac{k(k+1)}{2}$, we need to find, for each $\ell \in \{1,\ldots,r_k\}$, constants $\{\alpha_j^\ell\}_{j=1}^{2d_k}$ such that

$$\mathbf{q}_\ell^K \;:=\; \sum_{j=1}^{2d_k} \alpha_j^\ell\, \boldsymbol{\psi}_j^K \quad \text{and} \quad \int_K \nabla\varphi_{i+1}^K \cdot \mathbf{q}_\ell^K \;=\; 0 \quad \forall\, i \in \{1,\ldots,m_k - 1\}\,.$$

Equivalently, we have to solve the local rectangular linear systems

$$\mathbf{M}_K\, \mathbf{A}_K \;=\; \mathbf{0}\,, \tag{3.7}$$

where $\mathbf{0}$ is the null matrix in $\mathrm{R}^{(m_k-1)\times r_k}$, and the matrices $\mathbf{M}_K := (M_{ij,K}) \in \mathrm{R}^{(m_k-1)\times(2d_k)}$ and $\mathbf{A}_K := (A_{j\ell,K}) \in \mathrm{R}^{(2d_k)\times r_k}$ are given by

$$M_{ij,K} := \int_K \nabla\varphi_{i+1}^K \cdot \boldsymbol{\psi}_j^K \qquad \text{and} \qquad A_{j\ell,K} := \alpha_j^\ell \,,$$

respectively, $\forall\, i \in \{1,\ldots,m_k-1\}$, $\forall\, j \in \{1,\ldots,2d_k\}$, and $\forall\, \ell \in \{1,\ldots,r_k\}$. In this regard, the QR decomposition with column pivoting is employed to solve each system (3.7).

3.3 L^2-orthogonal projections, interpolants, and approximation properties

We now let $P_k^K : \mathrm{L}^2(K) \to \mathrm{P}_k(K)$ and $\mathcal{P}_k^K : \mathbf{L}^2(K) \to \mathbf{P}_k(K)$ be the orthogonal projector and its corresponding vectorial version, which, given $v \in \mathrm{L}^2(K)$ and $\mathbf{v} \in \mathbf{L}^2(K)$, are characterized by

$$P_k^K(v) \in \mathrm{P}_k(K) \quad \text{and} \quad \int_K P_k^K(v)\, q \,=\, \int_K v\, q \qquad \forall\, q \in \mathrm{P}_k(K) \tag{3.8}$$

and

$$\mathcal{P}_k^K(\mathbf{v}) \in \mathbf{P}_k(K) \quad \text{and} \quad \int_K \mathcal{P}_k^K(\mathbf{v}) \cdot \mathbf{q} \,=\, \int_K \mathbf{v} \cdot \mathbf{q} \qquad \forall\, \mathbf{q} \in \mathbf{P}_k(K)\,, \tag{3.9}$$

respectively. In addition, it is well-known (see, e.g. [9, eq. (22)] or [17, Lemma 3.4]) that, given an integer $m \in \big\{0,1,\ldots,k+1\big\}$, there hold the following approximation properties:

$$\|v - P_k^K(v)\|_{0,K} \;\le\; C\, h_K^m\, |v|_{m,K} \qquad \forall\, K \in \mathcal{T}_h\,, \quad \forall\, v \in \mathrm{H}^m(K)\,, \tag{3.10}$$

and

$$\|\mathbf{v} - \mathcal{P}_k^K(\mathbf{v})\|_{0,K} \;\le\; C\, h_K^m\, |\mathbf{v}|_{m,K} \qquad \forall\, K \in \mathcal{T}_h\,, \quad \forall\, \mathbf{v} \in \mathbf{H}^m(K)\,. \tag{3.11}$$

Actually, (3.11) is a direct consequence of (3.10) since it is easy to see that $\mathcal{P}_k^K(\mathbf{v}) \,=\, \big(P_k^K(v_1), P_k^K(v_2)\big)$ for all $\mathbf{v} := (v_1, v_2) \in \mathbf{H}^m(K)$.

At this point we observe for later use, as it was remarked in [9, Section 3.2], that the degrees of freedom given by (3.4) do allow the explicit calculation of $\mathcal{P}_k^K(\tau)$ for each $\tau \in \mathbf{H}_k^K$. Indeed, it suffices to check that the right-hand side of (3.9) is calculable in this case. To do that, we first note, thanks to the definitions of $m_{q,e}^{\boldsymbol{n}}(\tau)$ and $m_{q,K}^{\mathrm{div}}(\tau)$ (cf. (3.4)), that we can compute the value of $\mathrm{div}(\tau) \in \mathrm{P}_k(K)$ by using the identity

$$\int_K \mathrm{div}(\tau)\, q \,=\, -\int_K \tau \cdot \nabla q \,+\, \int_{\partial K} \tau \cdot \boldsymbol{n}\, q \qquad \forall\, q \in \mathrm{P}_k(K)\,. \tag{3.12}$$

Next, given $\mathbf{q} \in \mathbf{P}_k(K)$, we know that there exist unique $\mathbf{q}^\perp \in \big(\nabla \mathrm{P}_{k+1}(K)\big)^\perp \cap \mathbf{P}_k(K)$ and $\widetilde{q} \in \mathrm{P}_{k+1}(K)$, such that $\mathbf{q} = \mathbf{q}^\perp + \nabla\widetilde{q}$. In this way, it follows that

$$\int_K \tau \cdot \mathbf{q} \,=\, \int_K \tau \cdot \mathbf{q}^\perp \,+\, \int_K \tau \cdot \nabla\widetilde{q} \,=\, \int_K \tau \cdot \mathbf{q}^\perp \,-\, \int_K \widetilde{q}\, \mathrm{div}(\tau) \,+\, \int_{\partial K} \tau \cdot \boldsymbol{n}\, \widetilde{q}\,,$$

which, according to (3.12) and the definition of $m_{\mathbf{q},K}^{\mathrm{rot}}(\tau)$ (cf. (3.4)), yield the required calculation.

Furthermore, we now let $\Pi_k^K : \mathbf{H}^1(K) \to \mathbf{H}_k^K$ be the interpolation operator with respect to the degrees of freedom (3.4), that is, given $\tau \in \mathbf{H}^1(K)$, $\Pi_k^K(\tau)$ is the unique element in $\mathbf{H}_k^K$ such that

$$\begin{aligned}
m_{q,e}^{\boldsymbol{n}}(\Pi_k^K(\tau)) \;&:=\; \int_e \tau \cdot \boldsymbol{n}\, q \quad \forall\; q \in \mathcal{B}_k(e)\,, \quad \forall \text{ edge } e \in \partial K\,,\\
m_{q,K}^{\mathrm{div}}(\Pi_k^K(\tau)) \;&:=\; \int_K \tau \cdot \nabla q \quad \forall\; q \in \mathcal{B}_k(K) \setminus \{1\}\,,\\
m_{\mathbf{q},K}^{\mathrm{rot}}(\Pi_k^K(\tau)) \;&:=\; \int_K \tau \cdot \mathbf{q} \qquad \forall\; \mathbf{q} \in \mathcal{G}_k(K)\,.
\end{aligned}$$

Concerning the approximation properties of Π_k^K, we first recall from [9, eq. (28)] that for each $\tau \in \mathbf{H}^m(K)$, with $1 \leq m \leq k+1$, there holds

$$\|\tau - \Pi_k^K(\tau)\|_{0,K} \ \leq \ C\, h_K^m\, |\tau|_{m,K} \qquad \forall\, K \in \mathcal{T}_h\,. \tag{3.13}$$

In addition, for each $q \in \mathrm{P}_k(K)$ we find that

$$\int_K \mathrm{div}\big(\tau - \Pi_k^K(\tau)\big)\, q \ = \ -\int_K \big(\tau - \Pi_k^K(\tau)\big) \cdot \nabla q \ + \ \int_{\partial K} \big(\tau - \Pi_k^K(\tau)\big) \cdot \boldsymbol{n}\, q \ = \ 0\,,$$

which, thanks to the fact that $\mathrm{div}(\Pi_k^K(\tau)) \in \mathrm{P}_k(K)$, implies that

$$\mathrm{div}(\Pi_k^K(\tau)) \ = \ P_k^K(\mathrm{div}(\tau))\,. \tag{3.14}$$

In this way, applying (3.10) we deduce that for each $\tau \in \mathbf{H}^1(K)$, such that $\mathrm{div}(\tau) \in \mathrm{H}^m(K)$, with $0 \leq m \leq k+1$, there holds

$$\|\mathrm{div}(\tau - \Pi_k^K(\tau))\|_{0,K} \ \leq \ C\, h_K^m\, |\mathrm{div}(\tau)|_{m,K} \quad \forall\, K \in \mathcal{T}_h\,, \tag{3.15}$$

which, together with (3.13), show that for each $\tau \in \mathbf{H}^m(K)$ such that $\mathrm{div}(\tau) \in \mathrm{H}^m(K)$, with $1 \leq m \leq k+1$, there holds

$$\|\tau - \Pi_k^K(\tau)\|_{\mathrm{div};K} \ \leq \ C\, h_K^m \Big\{ |\tau|_{m,K} \ + \ |\mathrm{div}(\tau)|_{m,K} \Big\} \qquad \forall\, K \in \mathcal{T}_h\,. \tag{3.16}$$

Analogously, we now let $\boldsymbol{\Pi}_k^K : \mathbb{H}^1(K) \to \mathbb{H}_k^K$ (cf. (3.5)) be the interpolation operator with respect to the degrees of freedom (3.6). Then, it is straightforward to see that $\boldsymbol{\Pi}_k^K$ reduces to Π_k^K acting along each row of a tensor $\boldsymbol{\tau} \in \mathbb{H}^1(K)$, and hence, thanks to (3.16), we conclude now that for each $\boldsymbol{\tau} \in \mathbb{H}^m(K)$ such that $\mathbf{div}(\boldsymbol{\tau}) \in \mathbf{H}^m(K)$, with $1 \leq m \leq k+1$, there holds

$$\|\boldsymbol{\tau} - \boldsymbol{\Pi}_k^K(\boldsymbol{\tau})\|_{\mathbf{div};K} \ \leq \ C\, h_K^m \Big\{ |\boldsymbol{\tau}|_{m,K} \ + \ |\mathbf{div}(\boldsymbol{\tau})|_{m,K} \Big\} \qquad \forall\, K \in \mathcal{T}_h\,. \tag{3.17}$$

3.4 The conforming global virtual element subspaces

We now set the global virtual element subspaces of $\mathbf{H}(\mathrm{div};\Omega)$ and $\mathbb{H}(\mathbf{div};\Omega)$, respectively, that is

$$\mathbf{H}_k^h \ := \ \Big\{ \tau \in \mathbf{H}(\mathrm{div};\Omega) : \quad \tau|_K \in \mathbf{H}_k^K \quad \forall\, K \in \mathcal{T}_h \Big\}$$

and

$$\mathbb{H}_k^h \ := \ \Big\{ \boldsymbol{\tau} \in \mathbb{H}(\mathbf{div};\Omega) : \quad \boldsymbol{\tau}|_K \in \mathbb{H}_k^K \quad \forall\, K \in \mathcal{T}_h \Big\}\,, \tag{3.18}$$

or, equivalently

$$\mathbb{H}_k^h \ := \ \Big\{ \boldsymbol{\tau} \in \mathbb{H}(\mathbf{div};\Omega) : \quad (\tau_{i1},\, \tau_{i2})^{\mathtt{t}} \ \in \ \mathbf{H}_k^h \quad \forall\, i \in \{1,2\} \Big\}\,. \tag{3.19}$$

Then, we introduce the global interpolation operators $\Pi_k^h : \mathbf{H}^1(\Omega) \to \mathbf{H}_k^h$ and $\boldsymbol{\Pi}_k^h : \mathbb{H}^1(\Omega) \to \mathbb{H}_k^h$, whose local restrictions are given for each $K \in \mathcal{T}_h$ by

$$\Pi_k^h(\tau)|_K \ := \ \Pi_k^K(\tau|_K) \quad \forall\, \tau \in \mathbf{H}^1(\Omega) \qquad \text{and} \qquad \boldsymbol{\Pi}_k^h(\boldsymbol{\tau})|_K \ := \ \boldsymbol{\Pi}_k^K(\boldsymbol{\tau}|_K) \quad \forall\, \boldsymbol{\tau} \in \mathbb{H}^1(\Omega)\,.$$

Note that the well-definiteness of Π_k^h (resp. $\boldsymbol{\Pi}_k^h$) is guaranteed by the unisolvency in $\mathbf{H}_k^K$ (resp. $\mathbb{H}_k^K$) of the local degrees of freedom (3.4) (resp. (3.6)), and by the fact that the belonging $\Pi_k^h(\tau) \in \mathbf{H}(\mathrm{div};\Omega)$ (resp. $\boldsymbol{\Pi}_k^h(\boldsymbol{\tau}) \in \mathbb{H}(\mathbf{div};\Omega)$) follows from the definition of the degrees of freedom $m_{q,e}^{\boldsymbol{n}}$ (resp. $\mathbf{m}_{\mathbf{q},e}^{\boldsymbol{n}}$). Furthermore, we remark that the approximation properties of Π_k^h and $\boldsymbol{\Pi}_k^h$ follow straightforwardly from those of their local restrictions, which are given by (3.16) and (3.17), respectively.

4 The local discrete bilinear form

The purpose of this section is to define a computable discrete version $a_h^K : \mathbb{H}_h^K \times \mathbb{H}_h^K \to \mathrm{R}$ of the local bilinear form $a^K : \mathbb{H}(\mathbf{div}; K) \times \mathbb{H}(\mathbf{div}; K) \to \mathrm{R}$, which is given for each $K \in \mathcal{T}_h$ by

$$a^K(\boldsymbol{\zeta}, \boldsymbol{\tau}) := \frac{1}{\mu} \int_K \boldsymbol{\zeta}^{\mathrm{d}} : \boldsymbol{\tau}^{\mathrm{d}} + \frac{1}{\alpha} \int_K \mathbf{div}(\boldsymbol{\zeta}) \cdot \mathbf{div}(\boldsymbol{\tau}) \qquad \forall\, \boldsymbol{\zeta}, \boldsymbol{\tau} \in \mathbb{H}(\mathbf{div}; K)\,. \tag{4.1}$$

Indeed, the aforementioned goal is motivated by the fact that a^K is not explicitly calculable for $\boldsymbol{\zeta}$, $\boldsymbol{\tau} \in \mathbb{H}_h^K$ since in general the deviatoric tensors $\boldsymbol{\zeta}^{\mathrm{d}}$ and $\boldsymbol{\tau}^{\mathrm{d}}$ are not known on each $K \in \mathcal{T}_h$. In order to overcome this difficulty, we first assume the existence of an abstract space $\widehat{\mathbb{H}}_k^K$ and a corresponding projector $\widehat{\Pi}_k^K : \mathbb{H}(\mathbf{div}; K) \to \widehat{\mathbb{H}}_k^K$, both satisfying suitable conditions, so that a_h^K is expressed later on in terms of these projections instead of the original elements of $\mathbb{H}_h^K$. Next, a special bilinear form depending on the degrees of freedom defining $\mathbf{H}_k^K$ and $\mathbb{H}_k^K$, and which is also utilized to define a_h^K, is introduced. Then, the explicit definition of a_h^K is provided, and its main boundedness and positivity properties are established. Finally, specific examples of $\widehat{\mathbb{H}}_k^K$ and $\widehat{\Pi}_k^K$ verifying the indicated conditions are described.

4.1 A suitable projection of the local virtual space

In what follows we assume that for each $K \in \mathcal{T}_h$ there exist a subspace $\widehat{\mathbb{H}}_k^K$ of $\mathbb{H}(\mathbf{div}; K)$ and a projection $\widehat{\Pi}_k^K : \mathbb{H}(\mathbf{div}; K) \to \widehat{\mathbb{H}}_k^K$ satisfying the following abstract assumptions:

(A.1) $\widehat{\mathbb{H}}_k^K \subseteq \mathbb{P}_\ell(K)$ for some integer $\ell \geq 0$,

(A.2) $\widehat{\Pi}_k^K(\boldsymbol{\zeta})$ is explicitly calculable $\forall\, \boldsymbol{\zeta} \in \mathbb{H}_h^K$,

(A.3) there exists $\widehat{C} > 0$, independent of K, such that

$$\|\widehat{\Pi}_k^K(\boldsymbol{\zeta})\|_{0,K} \leq \widehat{C}\, \|\boldsymbol{\zeta}\|_{\mathbf{div};K} \qquad \forall\, \boldsymbol{\zeta} \in \mathbb{H}(\mathbf{div}; K)\,,$$

(A.4) $\displaystyle\int_K (\widehat{\Pi}_k^K(\boldsymbol{\zeta}))^{\mathrm{d}} : (\widehat{\Pi}_k^K(\boldsymbol{\tau}))^{\mathrm{d}} = \int_K (\widehat{\Pi}_k^K(\boldsymbol{\zeta}))^{\mathrm{d}} : \boldsymbol{\tau}^{\mathrm{d}} \quad \forall\, \boldsymbol{\zeta}, \boldsymbol{\tau} \in \mathbb{H}(\mathbf{div}; K),$ and

(A.5) given an integer $1 \leq m \leq k+1$, there exists a constant $C > 0$, independent of K, such that

$$\|\boldsymbol{\zeta} - \widehat{\Pi}_k^K(\boldsymbol{\zeta})\|_{0,K} \leq C\, h_K^m\, |\boldsymbol{\zeta}|_{m,K}\,,$$

for all $\boldsymbol{\zeta} \in \mathbb{H}^m(K)$, or at least for all $\boldsymbol{\zeta} \in \mathbb{H}^m_{\nabla\mathbf{curl}}(K)$, where

$$\mathbb{H}^m_{\nabla\mathbf{curl}}(K) := \Big\{ \boldsymbol{\zeta} \in \mathbb{H}^m(K) : \quad \boldsymbol{\zeta}^{\mathrm{d}} = \nabla\mathbf{curl}(w) \quad \text{for some} \quad w \in \mathrm{H}^{m+2}(K) \Big\}\,. \tag{4.2}$$

According to these assumptions, we first observe that **(A.1)** and **(A.2)** guarantee that for each $\boldsymbol{\zeta} \in \mathbb{H}_h^K$, $\widehat{\Pi}_k^K(\boldsymbol{\zeta})$ is known in the whole K. In addition, thanks to **(A.3)** and **(A.4)** we can carry out the *a priori* error analysis (see Section 5.1 below) of our mixed virtual element scheme (5.3). Finally, we observe in advance that the assumption **(A.5)** is required to prove later on the optimal rates of convergence for the pseudostress variable $\boldsymbol{\sigma}$. To this regard, note from the first equation in (2.2) and the third equation in (2.1) that $\boldsymbol{\sigma}^{\mathrm{d}} = \mu\nabla\mathbf{u} \in \mathbb{L}^2(\Omega)$ and $\mathrm{div}(\mathbf{u}) = 0$, respectively. Thus, there exists $w \in \mathrm{H}^2(\Omega)$ such that $\mathbf{u} = \mathbf{curl}(w) := (\partial_{x_2} w,\, -\partial_{x_1} w)^{\mathtt{t}}$, and hence $\boldsymbol{\sigma}^{\mathrm{d}} = \mu\nabla\mathbf{curl}(w)$. These remarks have motivated, similarly as done in [17], the introduction of the space $\mathbb{H}^m_{\nabla\mathbf{curl}}(K)$.

4.2 The degrees of freedom-based bilinear form

We now consider $K \in \mathcal{T}_h$ and gather all the K-moments of a given $\tau \in \mathbf{H}^1(K)$ (cf. (3.4)) in the set $\{m_{i,K}(\tau)\}_{i=1}^{n_k^K}$. Then, as usual we let $\{\boldsymbol{\varphi}_{j,K}\}_{j=1}^{n_k^K}$ be the canonical basis of $\mathbf{H}_k^K$, that is, given $i \in \{1, 2, \ldots, n_k^K\}$, $\boldsymbol{\varphi}_{i,K}$ is the unique element in $\mathbf{H}_k^K$ such that

$$m_{j,K}(\boldsymbol{\varphi}_{i,K}) \;=\; \delta_{ij} \qquad \forall\, j \in \{1, 2, \ldots, n_k^K\}\,.$$

It follows easily that

$$\Pi_k^K(\tau) \;:=\; \sum_{j=1}^{n_k^K} m_{j,K}(\tau)\, \boldsymbol{\varphi}_{j,K}\,,$$

or equivalently, $\Pi_k^K(\tau)$ is the unique element in $\mathbf{H}_k^K$ such that

$$m_{j,K}\big(\Pi_k^K(\tau)\big) \;=\; m_{j,K}(\tau) \qquad \forall\, j \in \{1, 2, \ldots, n_k^K\}\,, \qquad \forall\, \tau \in \mathbf{H}^1(K)\,.$$

In particular, it is also clear that

$$\tau \;:=\; \sum_{j=1}^{n_k^K} m_{j,K}(\tau)\, \boldsymbol{\varphi}_{j,K} \qquad \forall\, \tau \in \mathbf{H}_k^K\,.$$

Now, for each $K \in \mathcal{T}_h$ we let $s^K : \mathbf{H}_k^K \times \mathbf{H}_k^K \to \mathrm{R}$ be the bilinear form associated with the identity matrix in $\mathrm{R}^{n_k^K \times n_k^K}$ with respect to the basis $\{\boldsymbol{\varphi}_{j,K}\}_{j=1}^{n_k^K}$ of $\mathbf{H}_k^K$, that is

$$s^K(\tau, \zeta) \;:=\; \sum_{i=1}^{n_k^K} m_{i,K}(\tau)\, m_{i,K}(\zeta) \qquad \forall\, \tau,\, \zeta \,\in\, \mathbf{H}_k^K\,. \tag{4.3}$$

In this regards we recall from [13, eqs. (45) and (104)] (see also [13, eq. (5.8)]) that there exist c_0, $c_1 > 0$, depending only on $C_{\mathcal{T}}$, such that

$$c_0\, \|\tau\|_{0,K}^2 \;\leq\; s^K(\tau, \tau) \;\leq\; c_1\, \|\tau\|_{0,K}^2 \quad \forall\, \tau \in \mathbf{H}_k^K\,, \quad \forall\, K \in \mathcal{T}_h\,. \tag{4.4}$$

Then, we let $\mathcal{S}^K : \mathbb{H}_h^K \times \mathbb{H}_h^K \to \mathrm{R}$ be the bilinear form associated with the degrees of freedom of $\mathbb{H}_h^K$ (cf. (3.6)), that is

$$\mathcal{S}^K(\boldsymbol{\tau},\, \boldsymbol{\zeta}) \;:=\; \sum_{i=1}^{2} s^K\big((\tau_{i1}, \tau_{i2})^{\mathtt{t}}, (\zeta_{i1}, \zeta_{i2})^{\mathtt{t}}\big) \qquad \forall\, \boldsymbol{\tau} := (\tau_{ij}),\, \boldsymbol{\zeta} := (\zeta_{ij}) \in \mathbb{H}_h^K\,, \tag{4.5}$$

which, due to (4.4), satisfies

$$c_0\, \|\boldsymbol{\tau}\|_{0,K}^2 \;\leq\; \mathcal{S}^K(\boldsymbol{\tau}, \boldsymbol{\tau}) \;\leq\; c_1\, \|\boldsymbol{\tau}\|_{0,K}^2 \qquad \forall\, \boldsymbol{\tau} \in \mathbb{H}_h^K\,, \quad \forall\, K \in \mathcal{T}_h\,. \tag{4.6}$$

4.3 The computable local discrete bilinear form

Having provided the above analysis, we now let $a_h^K : \mathbb{H}_h^K \times \mathbb{H}_h^K \to \mathrm{R}$ be the local discrete bilinear form given by

$$\begin{aligned} a_h^K(\boldsymbol{\zeta}, \boldsymbol{\tau}) \;:=\; & \frac{1}{\mu} \int_K (\widehat{\Pi}_k^K(\boldsymbol{\zeta}))^{\mathrm{d}} : (\widehat{\Pi}_k^K(\boldsymbol{\tau}))^{\mathrm{d}} \,+\, \frac{1}{\alpha} \int_K \mathbf{div}(\boldsymbol{\zeta}) \cdot \mathbf{div}(\boldsymbol{\tau}) \\ & +\quad \mathcal{S}^K(\boldsymbol{\zeta} - \widehat{\Pi}_k^K(\boldsymbol{\zeta}),\, \boldsymbol{\tau} - \widehat{\Pi}_k^K(\boldsymbol{\tau})) \qquad\qquad \forall\, \boldsymbol{\zeta},\, \boldsymbol{\tau} \in \mathbb{H}_h^K\,. \end{aligned} \tag{4.7}$$

Then, we have the following result, which is consequence of the properties of $\widehat{\Pi}_k^K$ and (4.6).

Lemma 4.1. *For each $K \in \mathcal{T}_h$, there holds*

$$a_h^K(\boldsymbol{\zeta},\boldsymbol{\tau}) \;=\; a^K(\boldsymbol{\zeta},\boldsymbol{\tau}) \qquad \forall\, \boldsymbol{\zeta} \in \widehat{\mathbb{H}}_k^K, \quad \forall\, \boldsymbol{\tau} \in \mathbb{H}_h^K\,, \tag{4.8}$$

and there exist constants α_1, $\alpha_2 > 0$, independent of h and K, such that for all $\boldsymbol{\zeta}$, $\boldsymbol{\tau} \in \mathbb{H}_h^K$ there hold

$$|a_h^K(\boldsymbol{\zeta},\boldsymbol{\tau})| \;\leq\; \alpha_1 \Big\{ \|\boldsymbol{\zeta}\|_{\mathbf{div};K} \|\boldsymbol{\tau}\|_{\mathbf{div};K} \,+\, \|\boldsymbol{\zeta} - \widehat{\Pi}_k^K(\boldsymbol{\zeta})\|_{0,K} \|\boldsymbol{\tau} - \widehat{\Pi}_k^K(\boldsymbol{\tau})\|_{0,K} \Big\}\,, \tag{4.9}$$

and

$$\alpha_2 \Big\{ \|\boldsymbol{\zeta}^{\mathrm{d}}\|_{0,K}^2 \,+\, \|\mathbf{div}(\boldsymbol{\zeta})\|_{0,K}^2 \Big\} \;\leq\; a_h^K(\boldsymbol{\zeta},\boldsymbol{\zeta}) \;\leq\; \alpha_1 \Big\{ \|\boldsymbol{\zeta}\|_{\mathbf{div};K}^2 \,+\, \|\boldsymbol{\zeta} - \widehat{\Pi}_k^K(\boldsymbol{\zeta})\|_{0,K}^2 \Big\}\,. \tag{4.10}$$

Proof. We proceed as in [17, Lemma 4.6]. Indeed, given $\boldsymbol{\zeta} \in \widehat{\mathbb{H}}_k^K$ and $\boldsymbol{\tau} \in \mathbb{H}_h^K$, we certainly have that $\widehat{\Pi}_k^K(\boldsymbol{\zeta}) = \boldsymbol{\zeta}$, and hence we deduce from (4.7) and **(A.4)** that

$$\begin{aligned} a_h^K(\boldsymbol{\zeta},\boldsymbol{\tau}) \;&=\; \frac{1}{\mu} \int_K (\widehat{\Pi}_k^K(\boldsymbol{\zeta}))^{\mathrm{d}} : (\widehat{\Pi}_k^K(\boldsymbol{\tau}))^{\mathrm{d}} \,+\, \frac{1}{\alpha} \int_K \mathbf{div}(\boldsymbol{\zeta}) \cdot \mathbf{div}(\boldsymbol{\tau}) \\ &=\; \frac{1}{\mu} \int_K (\widehat{\Pi}_k^K(\boldsymbol{\zeta}))^{\mathrm{d}} : \boldsymbol{\tau}^{\mathrm{d}} \,+\, \frac{1}{\alpha} \int_K \mathbf{div}(\boldsymbol{\zeta}) \cdot \mathbf{div}(\boldsymbol{\tau}) \\ &=\; \frac{1}{\mu} \int_K \boldsymbol{\zeta}^{\mathrm{d}} : \boldsymbol{\tau}^{\mathrm{d}} \,+\, \frac{1}{\alpha} \int_K \mathbf{div}(\boldsymbol{\zeta}) \cdot \mathbf{div}(\boldsymbol{\tau}) \;=\; a^K(\boldsymbol{\zeta},\boldsymbol{\tau})\,, \end{aligned}$$

which proves (4.8). Next, for the boundedness of a_h^K we apply the Cauchy-Schwarz inequality, the estimate **(A.3)**, and the upper bound in (4.6), to obtain

$$\begin{aligned} |a_h^K(\boldsymbol{\zeta},\boldsymbol{\tau})| \;&\leq\; \frac{1}{\mu} \|(\widehat{\Pi}_k^K(\boldsymbol{\zeta}))^{\mathrm{d}}\|_{0,K} \|(\widehat{\Pi}_k^K(\boldsymbol{\tau}))^{\mathrm{d}}\|_{0,K} \,+\, \frac{1}{\alpha} \|\mathbf{div}(\boldsymbol{\zeta})\|_{0,K} \|\mathbf{div}(\boldsymbol{\tau})\|_{0,K} \\ &\quad + \Big\{ \mathcal{S}^K(\boldsymbol{\zeta} - \widehat{\Pi}_k^K(\boldsymbol{\zeta}), \boldsymbol{\zeta} - \widehat{\Pi}_k^K(\boldsymbol{\zeta})) \Big\}^{1/2} \Big\{ \mathcal{S}^K(\boldsymbol{\tau} - \widehat{\Pi}_k^K(\boldsymbol{\tau}), \boldsymbol{\tau} - \widehat{\Pi}_k^K(\boldsymbol{\tau})) \Big\}^{1/2} \\ &\leq\; \frac{1}{\mu} \widehat{C}^2 \, \|\boldsymbol{\zeta}\|_{\mathbf{div};K} \|\boldsymbol{\tau}\|_{\mathbf{div};K} \,+\, \frac{1}{\alpha} \|\boldsymbol{\zeta}\|_{\mathbf{div};K} \|\boldsymbol{\tau}\|_{\mathbf{div};K} \,+\, c_1 \|\boldsymbol{\zeta} - \widehat{\Pi}_k^K(\boldsymbol{\zeta})\|_{0,K} \|\boldsymbol{\tau} - \widehat{\Pi}_k^K(\boldsymbol{\tau})\|_{0,K}\,, \end{aligned}$$

for all $\boldsymbol{\zeta}, \boldsymbol{\tau} \in \mathbb{H}_h^K$, which gives (4.9) with $\alpha_1 := \max\{\frac{1}{\mu}\widehat{C}^2 + \frac{1}{\alpha}, c_1\}$. Finally, concerning (4.10), it is clear that the corresponding upper bound follows from (4.9). In turn, applying the lower estimate in (4.6), we find that

$$\begin{aligned} \|\boldsymbol{\zeta}^{\mathrm{d}}\|_{0,K}^2 \,+\, \|\mathbf{div}(\boldsymbol{\zeta})\|_{0,K}^2 \;&\leq\; 2\,\|(\widehat{\Pi}_k^K(\boldsymbol{\zeta}))^{\mathrm{d}}\|_{0,K}^2 \,+\, \|\mathbf{div}(\boldsymbol{\zeta})\|_{0,K}^2 \,+\, 2\,\|(\boldsymbol{\zeta} - \widehat{\Pi}_k^K(\boldsymbol{\zeta}))^{\mathrm{d}}\|_{0,K}^2 \\ &\leq\; 2\mu \left(\frac{1}{\mu} \|(\widehat{\Pi}_k^K(\boldsymbol{\zeta}))^{\mathrm{d}}\|_{0,K}^2 \right) \,+\, \alpha \left(\frac{1}{\alpha} \|\mathbf{div}(\boldsymbol{\zeta})\|_{0,K}^2 \right) \,+\, \frac{2}{c_0} \Big(c_0 \|\boldsymbol{\zeta} - \widehat{\Pi}_k^K(\boldsymbol{\zeta})\|_{0,K}^2 \Big) \\ &\leq\; 2\mu \left(\frac{1}{\mu} \|(\widehat{\Pi}_k^K(\boldsymbol{\zeta}))^{\mathrm{d}}\|_{0,K}^2 \right) \,+\, \alpha \left(\frac{1}{\alpha} \|\mathbf{div}(\boldsymbol{\zeta})\|_{0,K}^2 \right) \,+\, \frac{2}{c_0} \, \mathcal{S}^K(\boldsymbol{\zeta} - \widehat{\Pi}_k^K(\boldsymbol{\zeta}), \boldsymbol{\zeta} - \widehat{\Pi}_k^K(\boldsymbol{\zeta}))\,, \end{aligned}$$

for all $\boldsymbol{\zeta} \in \mathbb{H}_h^K$, which yields the lower bound in (4.10) with $\alpha_2 := \max\{2\mu, \alpha, \frac{2}{c_0}\}^{-1}$. □

4.4 Two particular choices for $\widehat{\mathbb{H}}_k^K$ and $\widehat{\Pi}_k^K$

We now proceed to define two possible choices for $\widehat{\mathbb{H}}_k^K$ and the projection $\widehat{\Pi}_k^K : \mathbb{H}(\mathbf{div};K) \to \widehat{\mathbb{H}}_k^K$.

First choice

We first consider $\widehat{\mathbb{H}}_k^K := \mathbb{P}_k(K)$, which clearly satisfies **(A.1)**, and let $\widehat{\Pi}_k^K := \boldsymbol{\mathcal{P}}_k^K : \mathbb{L}^2(K) \to \mathbb{P}_k(K)$ be the $\mathbb{L}^2(K)$-orthogonal projection. In other words, $\boldsymbol{\mathcal{P}}_k^K$ stands for the operator $\mathcal{P}_k^K$ (cf. (3.9)) acting along each row of a tensor in $\mathbb{L}^2(K)$. It follows straightforwardly from Section 3.3 that $\boldsymbol{\mathcal{P}}_k^K$ satisfies the assumptions **(A.2)**, and **(A.3)** with $\widehat{C} = 1$, whereas **(A.5)** is simply the tensorial version of (3.11). For the remaining assumption we use the characterization of $\boldsymbol{\mathcal{P}}_k^K$ and the fact that for each $\boldsymbol{\rho} \in \mathbb{P}_k(K)$ there certainly holds $\boldsymbol{\rho}^{\mathrm{d}} \in \mathbb{P}_k(K)$. Thus, we find that

$$\int_K (\widehat{\Pi}_k^K(\boldsymbol{\zeta}))^{\mathrm{d}} : (\widehat{\Pi}_k^K(\boldsymbol{\tau}))^{\mathrm{d}} \;=\; \int_K \widehat{\Pi}_k^K(\boldsymbol{\tau}) : (\widehat{\Pi}_k^K(\boldsymbol{\zeta}))^{\mathrm{d}} \;=\; \int_K \boldsymbol{\tau} : (\widehat{\Pi}_k^K(\boldsymbol{\zeta}))^{\mathrm{d}} \;=\; \int_K (\widehat{\Pi}_k^K(\boldsymbol{\zeta}))^{\mathrm{d}} : \boldsymbol{\tau}^{\mathrm{d}}\,,$$

for all $\boldsymbol{\zeta}, \boldsymbol{\tau} \in \mathbb{H}_h^K$, which proves **(A.4)**.

Second choice

On the other hand, because of the identity $\boldsymbol{\sigma}^{\mathrm{d}} = \mu\,\nabla\mathbf{u}$, with $\mathrm{div}(\mathbf{u}) = 0$ in Ω (cf. (2.2)), we now suggest the same projection defined in [17, Section 4] for the linear Stokes problem. More precisely, we consider the subspace of $\mathbb{P}_k(K)$ given by

$$\widehat{\mathbb{H}}_k^K \;:=\; \widehat{\mathbb{H}}_{k,\nabla}^K \oplus \widehat{\mathbb{H}}_{k,\mathbb{I}}^K\,, \tag{4.11}$$

where

$$\widehat{\mathbb{H}}_{k,\nabla}^K \;:=\; \Big\{\nabla\mathbf{curl}(q) \;:\; q \in \mathrm{span}\{\mathbf{x}^\alpha \;:\; 2 \le |\alpha| \le k+2\} \subseteq \mathrm{P}_{k+2}(K)\Big\}$$

and

$$\widehat{\mathbb{H}}_{k,\mathbb{I}}^K \;:=\; \Big\{q\,\mathbb{I} \;:\; q \in \mathrm{P}_k(K)\Big\}\,.$$

Then, we recall from [17, Lemma 4.1] that there holds $\dim \widehat{\mathbb{H}}_k^K = (k+1)(k+4)$. In addition, it is easy to see from (4.11) that $\mathrm{tr}(\boldsymbol{\tau}) = 0$ for all $\boldsymbol{\tau} \in \widehat{\mathbb{H}}_{k,\nabla}^K$.

In turn, as explained in [17], the corresponding projection operator $\widehat{\Pi}_k^K : \mathbb{H}(\mathbf{div}; K) \to \widehat{\mathbb{H}}_k^K$ is defined in terms of the decomposition:

$$\widehat{\Pi}_k^K(\boldsymbol{\zeta}) \;:=\; \widehat{\boldsymbol{\zeta}}_\nabla \;+\; q_{\boldsymbol{\zeta}}\,\mathbb{I} \;+\; c_{\boldsymbol{\zeta}}\,\mathbb{I} \;\in\; \widehat{\mathbb{H}}_k^K\,, \tag{4.12}$$

where the components $\widehat{\boldsymbol{\zeta}}_\nabla \in \widehat{\mathbb{H}}_{k,\nabla}^K$, $q_{\boldsymbol{\zeta}} \in \widehat{\mathrm{P}}_k(K) := \mathrm{span}\{\mathbf{x}^\alpha \;:\; 1 \le |\alpha| \le k\}$, and $c_{\boldsymbol{\zeta}} \in \mathrm{R}$ are computed according to the following sequentially connected problems:

- find $\widehat{\boldsymbol{\zeta}}_\nabla \in \widehat{\mathbb{H}}_{k,\nabla}^K$ such that

$$\int_K \widehat{\boldsymbol{\zeta}}_\nabla : \boldsymbol{\tau} \;=\; \int_K \boldsymbol{\zeta} : \boldsymbol{\tau} \qquad \forall\, \boldsymbol{\tau} \in \widehat{\mathbb{H}}_{k,\nabla}^K\,, \tag{4.13a}$$

- find $q_{\boldsymbol{\zeta}} \in \widehat{\mathrm{P}}_k(K)$ such that

$$\int_K \mathbf{div}(q_{\boldsymbol{\zeta}}\,\mathbb{I}) \cdot \mathbf{div}(q\,\mathbb{I}) \;=\; \int_K \mathbf{div}(\boldsymbol{\zeta} - \widehat{\boldsymbol{\zeta}}_\nabla) \cdot \mathbf{div}(q\,\mathbb{I}) \qquad \forall\, q \in \widehat{\mathrm{P}}_k(K)\,, \tag{4.13b}$$

  and

- find $c_{\boldsymbol{\zeta}} \in \mathrm{R}$ such that

$$\int_K \mathrm{tr}(\widehat{\Pi}_k^K(\boldsymbol{\zeta})) \;=\; \int_K \mathrm{tr}(\boldsymbol{\zeta})\,. \tag{4.13c}$$

Regarding the above definition of $\widehat{\Pi}_k^K$, we first remark that the unique solvability of (4.13) was guaranteed in [17, Section 4]. In particular, note that having computed $\widehat{\boldsymbol{\zeta}}_\nabla \in \widehat{\mathbb{H}}_{k,\nabla}^K$ and then $q_{\boldsymbol{\zeta}} \in \widehat{\mathrm{P}}_k(K)$, the identity (4.13c) yields

$$c_{\boldsymbol{\zeta}} \,=\, \frac{1}{2|K|}\int_K \big\{\mathrm{tr}(\boldsymbol{\zeta}) \;-\; 2q_{\boldsymbol{\zeta}}\big\}\,. \tag{4.14}$$

Next, we check that the right-hand sides of (4.13) are indeed calculable when $\boldsymbol{\zeta}$ belongs to our virtual space $\mathbb{H}_h^K$ (cf. (3.5)). Firstly, for each $\boldsymbol{\tau} := \nabla\mathbf{curl}(q) \in \widehat{\mathbb{H}}_{k,\nabla}^K$ we have that

$$\int_K \boldsymbol{\zeta} : \boldsymbol{\tau} \;=\; \int_K \boldsymbol{\zeta} : \nabla\mathbf{curl}(q) \;=\; -\int_K \mathbf{curl}(q)\cdot\mathbf{div}(\boldsymbol{\zeta}) \;+\; \int_{\partial K} \boldsymbol{\zeta}\boldsymbol{n}\cdot\mathbf{curl}(q)\,,$$

which establishes that the right-hand side of (4.13a) can be explicitly computed for $\boldsymbol{\zeta} \in \mathbb{H}_h^K$. In turn, since $\mathbf{div}(\boldsymbol{\zeta}) \in \mathbf{P}_k(K)$ (cf. (3.5)) and $\widehat{\boldsymbol{\zeta}}_\nabla \in \mathbb{P}_k(K)$, it is quite clear that the right-hand side of (4.13b) is also calculable for each $q \in \widehat{\mathrm{P}}_k(K)$. Finally, for the right-hand side of (4.13c) we simply observe that

$$\int_K \mathrm{tr}(\boldsymbol{\zeta}) \;=\; \int_K \boldsymbol{\zeta} : \mathbb{I} \;=\; \int_K \boldsymbol{\zeta} : \nabla\mathbf{x} \;=\; -\int_K \mathbf{x}\cdot\mathbf{div}(\boldsymbol{\zeta}) \;+\; \int_{\partial K} \boldsymbol{\zeta}\boldsymbol{n}\cdot\mathbf{x}\,,$$

which, according to (3.5), is calculable as well.

Next, it is straightforward to check from (4.13) that $\widehat{\Pi}_k^K(\boldsymbol{\zeta}) = \boldsymbol{\zeta}$ for all $\boldsymbol{\zeta} \in \widehat{\mathbb{H}}_k^K$, which confirms that $\widehat{\Pi}_k^K$ is in fact a projector. Hence, from the above discussion we have that the second choice of $\widehat{\Pi}_k^K$ satisfies the assumptions **(A.1)** and **(A.2)**. For **(A.3)** and **(A.5)** we refer to [17, Lemma 4.2] and [17, Lemma 4.4], respectively. Finally, employing (4.12) and (4.13a) we find that for all $\boldsymbol{\zeta}$, $\boldsymbol{\tau} \in \mathbb{H}(\mathbf{div};K)$ there holds

$$\begin{aligned}\int_K (\widehat{\Pi}_k^K(\boldsymbol{\zeta}))^{\mathrm{d}} : (\widehat{\Pi}_k^K(\boldsymbol{\tau}))^{\mathrm{d}} \;&=\; \int_K \widehat{\boldsymbol{\zeta}}_\nabla : \widehat{\boldsymbol{\tau}}_\nabla \;=\; \int_K \widehat{\boldsymbol{\zeta}}_\nabla : \boldsymbol{\tau}\\ &=\; \int_K (\widehat{\Pi}_k^K(\boldsymbol{\zeta}))^{\mathrm{d}} : \boldsymbol{\tau} \;=\; \int_K (\widehat{\Pi}_k^K(\boldsymbol{\zeta}))^{\mathrm{d}} : \boldsymbol{\tau}^{\mathrm{d}}\,,\end{aligned}$$

which constitutes **(A.4)**.

5 The mixed virtual element scheme

According to the analysis from the foregoing sections, and given an integer $k \geq 0$, we now consider the virtual element subspace $\mathbb{H}_h$ of $\mathbb{H} := \mathbb{H}_0(\mathbf{div};\Omega)$ given by

$$\mathbb{H}_h \;:=\; \mathbb{H}_k^h \,\cap\, \mathbb{H}_0(\mathbf{div};\Omega)\,, \tag{5.1}$$

where $\mathbb{H}_k^h$ is defined in (3.18) (or (3.19)) . Next, as suggested by (4.7), we define the global discrete bilinear form $a_h : \mathbb{H}_h \times \mathbb{H}_h \to \mathrm{R}$ as

$$a_h(\boldsymbol{\zeta},\boldsymbol{\tau}) \;:=\; \sum_{K\in\mathcal{T}_h} a_h^K(\boldsymbol{\zeta},\boldsymbol{\tau}) \qquad \forall\, \boldsymbol{\zeta},\boldsymbol{\tau} \in \mathbb{H}_h\,. \tag{5.2}$$

Then, the Galerkin scheme associated with (2.5) reads: Find $\boldsymbol{\sigma}_h \in \mathbb{H}_h$ such that

$$a_h(\boldsymbol{\sigma}_h,\boldsymbol{\tau}_h) \,=\, F(\boldsymbol{\tau}_h) \,:=\, -\frac{1}{\alpha}\int_\Omega \mathbf{f}\cdot\mathbf{div}(\boldsymbol{\tau}_h) \;+\; \langle\boldsymbol{\tau}_h\boldsymbol{n},\mathbf{g}\rangle_\Gamma \qquad \forall\, \boldsymbol{\tau}_h \in \mathbb{H}_h\,. \tag{5.3}$$

5.1 Solvability and a priori error analysis

The following result provides the discrete analogue of Lemma 2.2.

Lemma 5.1. *There exists $\eta > 0$, independent of h, such that*

$$a_h(\boldsymbol{\zeta}_h, \boldsymbol{\zeta}_h) \;\geq\; \eta \, \|\boldsymbol{\zeta}_h\|^2_{\mathbf{div};\Omega} \qquad \forall\, \boldsymbol{\zeta}_h \in \mathbb{H}_h \,.$$

Proof. We adapt the proofs of [17, Lemma 5.2] and Lemma 2.2. Indeed, according to the definition of a_h (cf. (5.2)), we apply the lower bound in (4.10) and Lemma 2.1 to find that for each $\boldsymbol{\zeta}_h \in \mathbb{H}_h$ there holds

$$\begin{aligned} a_h(\boldsymbol{\zeta}_h, \boldsymbol{\zeta}_h) &= \sum_{K \in \mathcal{T}_h} a_h^K(\boldsymbol{\zeta}_h, \boldsymbol{\tau}_h) \\ &\geq\; \alpha_2 \Big\{ \|\boldsymbol{\zeta}_h^{\mathrm{d}}\|^2_{0,\Omega} \,+\, \|\mathbf{div}(\boldsymbol{\zeta}_h)\|^2_{0,\Omega} \Big\} \\ &\geq\; c_\Omega \frac{\alpha_2}{2} \|\boldsymbol{\zeta}_h\|^2_{0,\Omega} + \frac{\alpha_2}{2} \|\mathbf{div}(\boldsymbol{\zeta}_h)\|^2_{0,\Omega} \,, \end{aligned}$$

which yields the proof with $\eta := \frac{\alpha_2}{2} \min\{1, c_\Omega\}$. □

The unique solvability and stability of the actual Galerkin scheme (5.3) is established now.

Theorem 5.1. *There exists a unique $\boldsymbol{\sigma}_h \in \mathbb{H}_h$ solution of* (5.3)*, and there exists a positive constant C, independent of h, such that*

$$\|\boldsymbol{\sigma}_h\|_{\mathbf{div};\Omega} \;\leq\; C \Big\{ \|\mathbf{f}\|_{0,\Omega} \,+\, \|\mathbf{g}\|_{1/2,\Gamma} \Big\} .$$

Proof. The boundedness of $a_h : \mathbb{H}_h \times \mathbb{H}_h \to \mathrm{R}$ with respect to the norm $\|\cdot\|_{\mathbf{div};\Omega}$ of $\mathbb{H}$ follows easily from (4.9) and **(A.3)**. Hence Lemma 5.1 and a straightforward application of the Lax-Milgram lemma complete the proof. □

We now aim to derive the corresponding *a priori* error estimates for (5.3) and (2.5). For this purpose, we will make use of the global interpolation operator $\boldsymbol{\Pi}_k^h : \mathbb{H}^1(\Omega) \to \mathbb{H}_k^h$ (cf. Section 3.4), whose local restriction is denoted $\boldsymbol{\Pi}_k^K : \mathbb{H}^1(K) \to \mathbb{H}_k^K$. In turn, given the local projector $\widehat{\boldsymbol{\Pi}}_k^K : \mathbb{H}(\mathbf{div}; K) \to \widehat{\mathbb{H}}_k^K$ defined by the assumptions **(A.1)** - **(A.5)**, we denote by $\widehat{\boldsymbol{\Pi}}_k^h$ its global counterpart, that is we let

$$\widehat{\boldsymbol{\Pi}}_k^h(\boldsymbol{\zeta})|_K \;:=\; \widehat{\boldsymbol{\Pi}}_k^K(\boldsymbol{\zeta}|_K) \qquad \forall\, K \in \mathcal{T}_h \,, \qquad \forall\, \boldsymbol{\zeta} \in \mathbb{H} \,.$$

Then, we have the following main result.

Theorem 5.2. *Let $\boldsymbol{\sigma} \in \mathbb{H}$ and $\boldsymbol{\sigma}_h \in \mathbb{H}_h$ be the unique solutions of the continuous and discrete schemes* (2.5) *and* (5.3)*, respectively. Then, there exists a positive constant C, independent of h, such that*

$$\|\boldsymbol{\sigma} - \boldsymbol{\sigma}_h\|_{\mathbf{div};\Omega} \;\leq\; C \Big\{ \|\boldsymbol{\sigma} - \boldsymbol{\Pi}_k^h(\boldsymbol{\sigma})\|_{\mathbf{div};\Omega} \,+\, \|\boldsymbol{\sigma} - \widehat{\boldsymbol{\Pi}}_k^h(\boldsymbol{\sigma})\|_{0,\Omega} \Big\} . \tag{5.4}$$

Proof. We adapt the proof of [17, Theorem 5.2]. Indeed, we first observe, thanks to the triangle inequality, that

$$\|\boldsymbol{\sigma} - \boldsymbol{\sigma}_h\|_{\mathbf{div};\Omega} \;\leq\; \|\boldsymbol{\sigma} - \boldsymbol{\Pi}_k^h(\boldsymbol{\sigma})\|_{\mathbf{div};\Omega} \,+\, \|\boldsymbol{\Pi}_k^h(\boldsymbol{\sigma}) - \boldsymbol{\sigma}_h\|_{\mathbf{div};\Omega} \,, \tag{5.5}$$

whence it only remains to estimate $\boldsymbol{\delta}_h := \boldsymbol{\Pi}_k^h(\boldsymbol{\sigma}) - \boldsymbol{\sigma}_h \in \mathbb{H}_h$. Hence, applying Lemma 5.1, adding and subtracting $\widehat{\boldsymbol{\Pi}}_k^h(\boldsymbol{\sigma})$, using the discrete and continuous formulations (5.3) and (2.5), respectively, employing (4.8), and finally utilizing the definitions of a_h^K and a^K (cf. (4.7), (4.1)), we find that

$$
\begin{aligned}
\eta\,\|\boldsymbol{\delta}_h\|^2_{\mathbf{div};\Omega} \;&\leq\; a_h(\boldsymbol{\delta}_h,\boldsymbol{\delta}_h) \;=\; a_h(\boldsymbol{\Pi}^h_k(\boldsymbol{\sigma}),\boldsymbol{\delta}_h) \,-\, a_h(\boldsymbol{\sigma}_h,\boldsymbol{\delta}_h)\\
&=\; a_h(\boldsymbol{\Pi}^h_k(\boldsymbol{\sigma})-\widehat{\Pi}^h_k(\boldsymbol{\sigma}),\boldsymbol{\delta}_h) \,+\, a_h(\widehat{\Pi}^h_k(\boldsymbol{\sigma}),\boldsymbol{\delta}_h) \,-\, a(\boldsymbol{\sigma},\boldsymbol{\delta}_h)\\
&=\; \sum_{K\in\mathcal{T}_h}\Big\{a^K_h(\boldsymbol{\Pi}^K_k(\boldsymbol{\sigma})-\widehat{\Pi}^K_k(\boldsymbol{\sigma}),\boldsymbol{\delta}_h) \,+\, a^K(\widehat{\Pi}^K_k(\boldsymbol{\sigma})-\boldsymbol{\sigma},\boldsymbol{\delta}_h)\Big\}\\
&=\; \sum_{K\in\mathcal{T}_h}\Big\{\frac{1}{\mu}\int_K \big(\widehat{\Pi}^K_k\{\boldsymbol{\Pi}^K_k(\boldsymbol{\sigma})-\boldsymbol{\sigma}\}\big)^{\mathrm{d}} : \big(\widehat{\Pi}^K_k(\boldsymbol{\delta}_h)\big)^{\mathrm{d}} \,+\, \frac{1}{\mu}\int_K \big(\widehat{\Pi}^K_k(\boldsymbol{\sigma})-\boldsymbol{\sigma}\big)^{\mathrm{d}} : \boldsymbol{\delta}^{\mathrm{d}}_h\\
&\quad +\,\frac{1}{\alpha}\int_K \mathbf{div}(\boldsymbol{\Pi}^K_k(\boldsymbol{\sigma})-\boldsymbol{\sigma})\cdot\mathbf{div}(\boldsymbol{\delta}_h) \,+\, \mathcal{S}^K\big(\boldsymbol{\Pi}^K_k(\boldsymbol{\sigma})-\widehat{\Pi}^K_k\{\boldsymbol{\Pi}^K_k(\boldsymbol{\sigma})\},\boldsymbol{\delta}_h-\widehat{\Pi}^K_k(\boldsymbol{\delta}_h)\big)\Big\}\,.
\end{aligned}
$$

In addition, applying the Cauchy-Schwarz inequality, the upper bound from (4.6), and the estimate provided by the assumption **(A.3)**, we obtain, with the constant $C := \frac{1}{\eta}\max\{\frac{1}{\mu}\widehat{C}^2+\frac{1}{\alpha},\frac{1}{\mu},c_1(1+\widehat{C})\}$, that

$$
\|\boldsymbol{\delta}_h\|^2_{\mathbf{div};\Omega} \;\leq\; C\Big\{\|\boldsymbol{\sigma}-\boldsymbol{\Pi}^h_k(\boldsymbol{\sigma})\|_{\mathbf{div};\Omega} \,+\, \|\boldsymbol{\sigma}-\widehat{\Pi}^h_k(\boldsymbol{\sigma})\|_{0,\Omega} \,+\, \|\boldsymbol{\Pi}^h_k(\boldsymbol{\sigma})-\widehat{\Pi}^h_k\{\boldsymbol{\Pi}^h_k(\boldsymbol{\sigma})\}\|_{0,\Omega}\Big\}\|\boldsymbol{\delta}_h\|_{\mathbf{div};\Omega}\,,
$$

which yields

$$
\|\boldsymbol{\delta}_h\|_{\mathbf{div};\Omega} \;\leq\; C\Big\{\|\boldsymbol{\sigma}-\boldsymbol{\Pi}^h_k(\boldsymbol{\sigma})\|_{\mathbf{div};\Omega} \,+\, \|\boldsymbol{\sigma}-\widehat{\Pi}^h_k(\boldsymbol{\sigma})\|_{0,\Omega} \,+\, \|\boldsymbol{\Pi}^h_k(\boldsymbol{\sigma})-\widehat{\Pi}^h_k\{\boldsymbol{\Pi}^h_k(\boldsymbol{\sigma})\}\|_{0,\Omega}\Big\}\,. \tag{5.6}
$$

Next, adding and subtracting $\boldsymbol{\sigma}-\widehat{\Pi}^h_k(\boldsymbol{\sigma})$, and employing again the boundedness of $\widehat{\Pi}^K_k$ (cf. **(A.3)**), we deduce that

$$
\begin{aligned}
\|\boldsymbol{\Pi}^h_k(\boldsymbol{\sigma})-\widehat{\Pi}^h_k\{\boldsymbol{\Pi}^h_k(\boldsymbol{\sigma})\}\|_{0,\Omega} \;&\leq\; \|\boldsymbol{\sigma}-\boldsymbol{\Pi}^h_k(\boldsymbol{\sigma})\|_{0,\Omega} \,+\, \|\boldsymbol{\sigma}-\widehat{\Pi}^h_k(\boldsymbol{\sigma})\|_{0,\Omega} \,+\, \|\widehat{\Pi}^h_k\{\boldsymbol{\sigma}-\boldsymbol{\Pi}^h_k(\boldsymbol{\sigma})\}\|_{0,\Omega}\\
&\leq\; \big(1+\widehat{C}\big)\Big\{\|\boldsymbol{\sigma}-\boldsymbol{\Pi}^h_k(\boldsymbol{\sigma})\|_{\mathbf{div};\Omega} \,+\, \|\boldsymbol{\sigma}-\widehat{\Pi}^h_k(\boldsymbol{\sigma})\|_{0,\Omega}\Big\}\,,
\end{aligned}
$$

which, together with (5.6) and (5.5), imply the estimate (5.4) and complete the proof. □

Having established the *a priori* error estimates for our unknown, we now provide the corresponding rate of convergence. Recall from (4.2) the definition of the space $\mathbb{H}^r_{\nabla\mathbf{curl}}(K)$.

Theorem 5.3. *Let $\boldsymbol{\sigma}\in\mathbb{H}$ and $\boldsymbol{\sigma}_h\in\mathbb{H}_h$ be the unique solutions of the continuous and discrete schemes* (2.5) *and* (5.3)*, respectively. Assume that for some $r\in[1,k+1]$ there hold $\boldsymbol{\sigma}|_K\in\mathbb{H}^r_{\nabla\mathbf{curl}}(K)\subseteq\mathbb{H}^r(K)$ and $\mathbf{div}(\boldsymbol{\sigma})|_K\in\mathbf{H}^r(K)$ for each $K\in\mathcal{T}_h$. Then, there exists a positive constant C, independent of h, such that*

$$
\|\boldsymbol{\sigma}-\boldsymbol{\sigma}_h\|_{\mathbf{div};\Omega} \;\leq\; C\,h^r\sum_{K\in\mathcal{T}_h}\Big\{|\boldsymbol{\sigma}|_{r,K} \,+\, |\mathbf{div}(\boldsymbol{\sigma})|_{r,K}\Big\}\,. \tag{5.7}
$$

Proof. It follows from (5.4) and a straightforward application of the approximation properties provided by (3.16) and **(A.5)**. □

5.2 Computable approximations of $\boldsymbol{\sigma}$, p, and $\mathbf{u}$

We now introduce the fully computable approximation of $\boldsymbol{\sigma}_h$ given by

$$
\widehat{\boldsymbol{\sigma}}_h \;:=\; \widehat{\Pi}^h_k(\boldsymbol{\sigma}_h)\,, \tag{5.8}
$$

and establishes next the corresponding *a priori* error estimate in the $\mathbb{L}^2(\Omega)$-norm, which, as shown below in Theorem 5.4, yields exactly the same rate of convergence given by Theorem 5.3.

Lemma 5.2. *There exists a positive constant C, independent of h, such that*

$$\|\boldsymbol{\sigma}-\widehat{\boldsymbol{\sigma}}_h\|_{0,\Omega} \;\leq\; C\Big\{\|\boldsymbol{\sigma}-\boldsymbol{\Pi}_k^h(\boldsymbol{\sigma})\|_{\mathbf{div};\Omega} \;+\; \|\boldsymbol{\sigma}-\widehat{\Pi}_k^h(\boldsymbol{\sigma})\|_{0,\Omega}\Big\}\,. \tag{5.9}$$

Proof. Similarly as in [17, Theorem 5.4], we first write by triangle inequality that

$$\|\boldsymbol{\sigma}-\widehat{\boldsymbol{\sigma}}_h\|_{0,\Omega} \,\leq\, \|\boldsymbol{\sigma}-\boldsymbol{\sigma}_h\|_{0,\Omega} \,+\, \|\boldsymbol{\sigma}_h-\widehat{\Pi}_k^h(\boldsymbol{\sigma}_h)\|_{0,\Omega}\,. \tag{5.10}$$

Next, adding and subtracting $\boldsymbol{\sigma}$ and $\widehat{\Pi}_k^h(\boldsymbol{\sigma})$, and utilizing the boundedness of $\widehat{\Pi}_k^K$ (cf. **(A.3)**), we find that

$$\begin{aligned}\|\boldsymbol{\sigma}_h-\widehat{\Pi}_k^h(\boldsymbol{\sigma}_h)\|_{0,\Omega} \,&\leq\, \|\boldsymbol{\sigma}-\boldsymbol{\sigma}_h\|_{0,\Omega} \,+\, \|\boldsymbol{\sigma}-\widehat{\Pi}_k^h(\boldsymbol{\sigma})\|_{0,\Omega} \,+\, \|\widehat{\Pi}_k^h(\boldsymbol{\sigma}-\boldsymbol{\sigma}_h)\|_{0,\Omega}\\ &\leq\, C\,\Big\{\|\boldsymbol{\sigma}-\boldsymbol{\sigma}_h\|_{\mathbf{div};\Omega} \,+\, \|\boldsymbol{\sigma}-\widehat{\Pi}_k^h(\boldsymbol{\sigma})\|_{0,\Omega}\Big\}\,,\end{aligned} \tag{5.11}$$

which, replaced back into (5.10), and then combined with (5.4), gives (5.9) and completes the proof. □

We remark here that the lack of the approximation property of $\widehat{\Pi}_k^h$ in the whole $\mathbb{H}(\mathbf{div};K)$-norm does not allow us to establish an estimate for $\|\boldsymbol{\sigma}-\widehat{\boldsymbol{\sigma}}_h\|_{\mathbf{div};\Omega}$. Nevertheless, thanks to a suitable postprocessing of $\widehat{\boldsymbol{\sigma}}_h$, we are able to provide below (cf. Section 5.3) an explicitly calculable second approximation of $\boldsymbol{\sigma}$ yielding an optimal rate of convergence in the broken $\mathbb{H}(\mathbf{div})$-norm.

On the other hand, since we know from (2.3) that $p=-\frac{1}{2}\,\mathrm{tr}(\boldsymbol{\sigma})$, we now suggest to define the following approximation of the pressure:

$$p_h \,:=\, -\,\frac{1}{2}\,\mathrm{tr}(\widehat{\boldsymbol{\sigma}}_h)\,, \tag{5.12}$$

so that there holds

$$\|p-p_h\|_{0,\Omega} \,=\, \frac{1}{2}\,\|\mathrm{tr}(\boldsymbol{\sigma}-\widehat{\boldsymbol{\sigma}}_h)\|_{0,\Omega} \,\leq\, \frac{1}{\sqrt{2}}\,\|\boldsymbol{\sigma}-\widehat{\boldsymbol{\sigma}}_h\|_{0,\Omega}\,,$$

which, together with (5.9), gives the *a priori* error estimate for the pressure, that is

$$\|p-p_h\|_{0,\Omega} \,\leq\, C\,\Big\{\|\boldsymbol{\sigma}-\boldsymbol{\Pi}_k^h(\boldsymbol{\sigma})\|_{\mathbf{div};\Omega} \,+\, \|\boldsymbol{\sigma}-\widehat{\Pi}_k^h(\boldsymbol{\sigma})\|_{0,\Omega}\Big\}\,. \tag{5.13}$$

In turn, resembling (2.4), we now set the approximation of $\mathbf{u}$ as

$$\mathbf{u}_h \,:=\, \frac{1}{\alpha}\big\{\mathcal{P}_k^h(\mathbf{f}) \,+\, \mathbf{div}(\boldsymbol{\sigma}_h)\big\}\,, \tag{5.14}$$

where $\mathcal{P}_k^h$ is the $\mathbf{L}^2(\Omega)$-orthogonal projector onto the space of piecewise polynomial vectors of degree $\leq k$. Equivalently, we can set $\mathcal{P}_k^h(\mathbf{v})|_K \,=\, \mathcal{P}_k^K(\mathbf{v}|_K)$ for each $K\in\mathcal{T}_h$, for all $\mathbf{v}\in\mathbf{L}^2(\Omega)$, where $\mathcal{P}_k^K:\mathbf{L}^2(K)\to\mathbf{P}_k(K)$ is the local orthogonal projector defined in (3.9). Hence, it readily follows from (2.4) and (5.14) that

$$\|\mathbf{u}-\mathbf{u}_h\|_{0,\Omega} \,\leq\, \frac{1}{\alpha}\,\Big\{\|\mathbf{f}-\mathcal{P}_k^h(\mathbf{f})\|_{0,\Omega} \,+\, \|\mathbf{div}(\boldsymbol{\sigma}-\boldsymbol{\sigma}_h)\|_{0,\Omega}\Big\}\,,$$

from which, using that $\mathbf{f}=\alpha\,\mathbf{u}-\mathbf{div}(\boldsymbol{\sigma})$ (cf. (2.1)), bounding $\|\mathbf{div}(\boldsymbol{\sigma}-\boldsymbol{\sigma}_h)\|_{0,\Omega}$ by $\|\boldsymbol{\sigma}-\boldsymbol{\sigma}_h\|_{\mathbf{div};\Omega}$, and employing the a priori error estimate (5.4) (cf. Theorem 5.2), we deduce that

$$\begin{aligned}\|\mathbf{u}-\mathbf{u}_h\|_{0,\Omega} \,&\leq\, C\,\Big\{\|\mathbf{u}-\mathcal{P}_k^h(\mathbf{u})\|_{0,\Omega} \,+\, \|\mathbf{div}(\boldsymbol{\sigma})-\mathcal{P}_k^h(\mathbf{div}(\boldsymbol{\sigma}))\|_{0,\Omega}\\ &\quad+\quad \|\boldsymbol{\sigma}-\boldsymbol{\Pi}_k^h(\boldsymbol{\sigma})\|_{\mathbf{div};\Omega} \,+\, \|\boldsymbol{\sigma}-\widehat{\Pi}_k^h(\boldsymbol{\sigma})\|_{0,\Omega}\Big\}\,.\end{aligned} \tag{5.15}$$

In this way, we are now able to provide the theoretical rates of convergence for $\widehat{\boldsymbol{\sigma}}_h$, p_h, and $\mathbf{u}_h$.

Theorem 5.4. *Let $\boldsymbol{\sigma} \in \mathbb{H}$ and $\boldsymbol{\sigma}_h \in \mathbb{H}_h$ be the unique solutions of the continuous and discrete schemes* (2.5) *and* (5.3)*, respectively. In addition, let $\widehat{\boldsymbol{\sigma}}_h$, p_h, and $\mathbf{u}_h$ be the discrete approximations introduced in* (5.8)*,* (5.12)*, and* (5.14)*, respectively. Assume that for some $r \in [1, k+1]$ there hold $\boldsymbol{\sigma}|_K \in \mathbb{H}^r_{\nabla\mathbf{curl}}(K) \subseteq \mathbb{H}^r(K)$, $\mathbf{div}(\boldsymbol{\sigma})|_K \in \mathbf{H}^r(K)$, and $\mathbf{u}|_K \in \mathbf{H}^r(K)$ for each $K \in \mathcal{T}_h$. Then, there exist positive constants C_1 and C_2, independent of h, such that*

$$\|\boldsymbol{\sigma} - \widehat{\boldsymbol{\sigma}}_h\|_{0,\Omega} \, + \, \|p - p_h\|_{0,\Omega} \, \leq \, C_1 \, h^r \sum_{K \in \mathcal{T}_h} \Big\{ |\boldsymbol{\sigma}|_{r,K} \, + \, |\mathbf{div}(\boldsymbol{\sigma})|_{r,K} \Big\} , \tag{5.16}$$

and

$$\|\mathbf{u} - \mathbf{u}_h\|_{0,\Omega} \, \leq \, C_2 \, h^r \sum_{K \in \mathcal{T}_h} \Big\{ |\boldsymbol{\sigma}|_{r,K} \, + \, |\mathbf{div}(\boldsymbol{\sigma})|_{r,K} \, + \, |\mathbf{u}|_{r,K} \Big\} . \tag{5.17}$$

Proof. It follows from (5.9), (5.13), (5.15), and a straightforward application of the approximation properties provided by (3.11), (3.16), and **(A.5)**. □

5.3 A convergent approximation of $\boldsymbol{\sigma}$ in the broken $\mathbb{H}(\mathbf{div})$-norm

Finally, motivated by the approach developed in [22, 23], we now construct a second approximation $\boldsymbol{\sigma}^\star_h$ of the pseudostress $\boldsymbol{\sigma}$, which is shown below to yield an optimal rate of convergence in the broken $\mathbb{H}(\mathbf{div})$-norm. To this end, we first consider for each $K \in \mathcal{T}_h$ an arbitrary finite dimensional subspace $\mathbb{V}(K)$ of $\mathbb{H}(\mathbf{div}; K)$, which is going to be suitably chosen later on. Then, we let $(\cdot,\cdot)_{\mathbf{div};K}$ be the usual $\mathbb{H}(\mathbf{div}; K)$-inner product with induced norm $\|\cdot\|_{\mathbf{div};K}$, and set $\boldsymbol{\sigma}^\star_h|_K := \boldsymbol{\sigma}^\star_{h,K} \in \mathbb{V}(K)$, where $\boldsymbol{\sigma}^\star_{h,K}$ is the unique solution of the local problem

$$(\boldsymbol{\sigma}^\star_{h,K}, \, \boldsymbol{\tau}_h)_{\mathbf{div};K} \, = \, \int_K \widehat{\boldsymbol{\sigma}}_h : \boldsymbol{\tau}_h \, + \, \int_K \mathbf{div}(\boldsymbol{\sigma}_h) \cdot \mathbf{div}(\boldsymbol{\tau}_h) \qquad \forall \, \boldsymbol{\tau}_h \in \mathbb{V}(K) \, . \tag{5.18}$$

We emphasize that $\boldsymbol{\sigma}^\star_{h,K}$ can be explicitly (and, if the definition of $\mathbb{V}(K)$ allows it, efficiently) calculated for each $K \in \mathcal{T}_h$, independently. Throughout the rest of the section we let $\Pi^K_V : \mathbb{H}(\mathbf{div}; K) \to \mathbb{V}(K)$ be the orthogonal projector with respect to $(\cdot,\cdot)_{\mathbf{div};K}$. Then, the following result establishes the *a priori* estimate for the local error $\|\boldsymbol{\sigma} - \boldsymbol{\sigma}^\star_{h,K}\|_{\mathbf{div};K}$.

Lemma 5.3. *For each $K \in \mathcal{T}_h$ there holds*

$$\|\boldsymbol{\sigma} - \boldsymbol{\sigma}^\star_{h,K}\|_{\mathbf{div};K} \, \leq \, \|\boldsymbol{\sigma} - \widehat{\boldsymbol{\sigma}}_h\|_{0,K} \, + \, \|\mathbf{div}(\boldsymbol{\sigma} - \boldsymbol{\sigma}_h)\|_{0,K} \, + \, \|\boldsymbol{\sigma} - \Pi^K_V(\boldsymbol{\sigma})\|_{\mathbf{div};K} \, . \tag{5.19}$$

Proof. We proceed as in the proof of [22, Lemma 3.1]. In fact, using the orthogonality condition $(\boldsymbol{\sigma} - \Pi^K_V(\boldsymbol{\sigma}), \boldsymbol{\tau}_h)_{\mathbf{div};K} = 0 \quad \forall \, \boldsymbol{\tau}_h \in \mathbb{V}(K)$, together with (5.18), we first obtain the error equation

$$(\Pi^K_V(\boldsymbol{\sigma}) - \boldsymbol{\sigma}^\star_{h,K}, \boldsymbol{\tau}_h)_{\mathbf{div};K} \, = \, \int_K (\boldsymbol{\sigma} - \widehat{\boldsymbol{\sigma}}_h) : \boldsymbol{\tau}_h \, + \, \int_K \mathbf{div}(\boldsymbol{\sigma} - \boldsymbol{\sigma}_h) \cdot \mathbf{div}(\boldsymbol{\tau}_h) \quad \forall \, \boldsymbol{\tau}_h \in \mathbb{V}(K) \, .$$

Then, taking in particular $\boldsymbol{\tau}_h := \Pi^K_V(\boldsymbol{\sigma}) - \boldsymbol{\sigma}^\star_{h,K} \in \mathbb{V}(K)$ in the foregoing identity, and then using the Cauchy-Schwarz and triangle inequalities, we arrive at (5.19), thus finishing the proof. □

At this point we notice from our previous analysis that the first two terms on the right-hand side of (5.19) converge at most with $O(h^{k+1})$, and hence we must choose $\mathbb{V}(K)$ so that at least this rate of convergence is guaranteed by the projection error $\|\boldsymbol{\sigma} - \Pi^K_V(\boldsymbol{\sigma})\|_{\mathbf{div};K}$ as well. According to it, and for simplicity, we now pick $\mathbb{V}(K) := \mathbb{P}_{k+1}(K)$, whence the resulting rate of convergence is given as follows.

Theorem 5.5. *Let $\boldsymbol{\sigma} \in \mathbb{H}$ and $\boldsymbol{\sigma}_h \in \mathbb{H}_h$ be the unique solutions of the continuous and discrete schemes* (2.5) *and* (5.3)*, respectively. In addition, let $\widehat{\boldsymbol{\sigma}}_h$ and $\boldsymbol{\sigma}_h^\star$ be the discrete approximations introduced in* (5.8) *and* (5.18) *with $\mathbb{V}(K) := \mathbb{P}_{k+1}(K)$, respectively. Assume that for some $r \in [1, k+1]$ there hold $\boldsymbol{\sigma}|_K \in \mathbb{H}^r_{\nabla\mathbf{curl}}(K) \subseteq \mathbb{H}^r(K)$ and $\mathbf{div}(\boldsymbol{\sigma})|_K \in \mathbf{H}^r(K)$ for each $K \in \mathcal{T}_h$. Then, there exists a positive constant C, independent of h, such that*

$$\left\{ \sum_{K\in\mathcal{T}_h} \|\boldsymbol{\sigma} - \boldsymbol{\sigma}_h^\star\|^2_{\mathbf{div};K} \right\}^{1/2} \leq C\, h^r \sum_{K\in\mathcal{T}_h} \left\{ |\boldsymbol{\sigma}|_{r,K} \ + \ |\mathbf{div}(\boldsymbol{\sigma})|_{r,K} \right\}. \tag{5.20}$$

Proof. Given $K \in \mathcal{T}_h$, we first let $\boldsymbol{\mathcal{P}}^K_{k+1} : \mathbb{L}^2(K) \to \mathbb{P}_{k+1}(K)$ be the $\mathbb{L}^2(K)$-orthogonal projector. Then, it readily follows that

$$\|\boldsymbol{\sigma} - \Pi^K_V(\boldsymbol{\sigma})\|_{\mathbf{div};K} \leq \|\boldsymbol{\sigma} - \boldsymbol{\mathcal{P}}^K_{k+1}(\boldsymbol{\sigma})\|_{\mathbf{div};K} \leq C \left\{ \|\boldsymbol{\sigma} - \boldsymbol{\mathcal{P}}^K_{k+1}(\boldsymbol{\sigma})\|_{0,K} \ + \ |\boldsymbol{\sigma} - \boldsymbol{\mathcal{P}}^K_{k+1}(\boldsymbol{\sigma})|_{1,K} \right\},$$

which, applying [17, Lemma 3.4], leads to $\|\boldsymbol{\sigma} - \Pi^K_V(\boldsymbol{\sigma})\|_{\mathbf{div};K} \leq C\, h_K^r\, |\boldsymbol{\sigma}|_{r,K}$. Next, replacing this estimate back into (5.19), summing the squares of the resulting (5.19) over all $K \in \mathcal{T}_h$, and employing the upper bounds for $\|\boldsymbol{\sigma} - \widehat{\boldsymbol{\sigma}}_h\|_{0,\Omega}$ and $\|\boldsymbol{\sigma} - \boldsymbol{\sigma}_h\|_{\mathbf{div};\Omega}$ provided by (5.16) (cf. Theorem 5.4) and (5.7) (cf. Theorem 5.3), respectively, we conclude (5.20) and end the proof. □

6 Numerical results

In this section we present two numerical examples illustrating the good performance of the mixed virtual finite element scheme (5.3) introduced and analyzed in Section 5. Here, we use both choices of $\widehat{\mathbb{H}}^K_k$ and $\widehat{\Pi}^K_k$ described in Section 4.4. More precisely, we utilize the $\mathbb{L}^2$-orthogonal projection and the projection defined by (4.13), which, according to the lastname initials of the authors of [17], is called from now on the $\mathbb{CG}$-projection. In turn, for all the computations we consider the virtual element subspace $\mathbb{H}_h$ given by (5.1) with $k \in \{0, 1, 2\}$. However, similarly as in [18], the zero integral mean condition for tensors in the space $\mathbb{H}_h$ is imposed via a real Lagrange multiplier. This means that (5.3) is reformulated, equivalently, as: Find $(\boldsymbol{\sigma}_h, \lambda) \in \mathbb{H}^h_k \times \mathrm{R}$ such that

$$\begin{array}{rcll} a_h(\boldsymbol{\sigma}_h, \boldsymbol{\tau}_h) \ + \ \lambda \displaystyle\int_\Omega \mathrm{tr}(\boldsymbol{\tau}_h) & = & F(\boldsymbol{\tau}_h) & \forall\, \boldsymbol{\tau}_h \in \mathbb{H}^h_k\,, \\ \xi \displaystyle\int_\Omega \mathrm{tr}(\boldsymbol{\sigma}_h) & = & 0 & \forall\, \xi \in \mathrm{R}\,. \end{array} \tag{6.1}$$

Note here that the constraint $\int_\Omega \mathrm{tr}(\boldsymbol{\sigma}_h) = 0$, which is automatically satisfied by the members of the subspace $\mathbb{H}_h$ (cf. (5.1)), is not incorporated in the definition of the space $\mathbb{H}^h_k$ where $\boldsymbol{\sigma}_h$ is sought now, but it is imposed weakly through the second equation of (6.1). In other words, λ is an artificial unknown acting as the Lagrange multiplier taking care of that condition, which, thanks to the compatibility assumption satisfied by $\mathbf{g}$, is known in advance to be 0. Nevertheless, λ is kept in (6.1) to guarantee the symmetry of this equivalent system. On the other hand, concerning the polygonal decompositions of Ω employed in our computations, we consider uniform triangles as well as distorted squares and hexagons (the latter being generated by PolyMesher [30] in Example 1).

Furthermore, in what follows, N stands for the total number of unknowns (d.o.f.) of (5.3), that is,

$$N \ := \ 2(k+1) \times \{\text{number of edges } e \in \mathcal{T}_h\} \ + \ 2k(k+2) \times \{\text{number of elements } K \in \mathcal{T}_h\} \ + \ 1\,,$$

whereas the individual errors are defined by

$$\mathsf{e}(\boldsymbol{\sigma}) \ := \ \|\boldsymbol{\sigma} - \widehat{\boldsymbol{\sigma}}_h\|_{0,\Omega}\,, \quad \mathsf{e}(p) \ := \ \|p - p_h\|_{0,\Omega}\,, \quad \mathsf{e}(\mathbf{u}) \ := \ \|\mathbf{u} - \mathbf{u}_h\|_{0,\Omega}\,,$$

and

$$\mathtt{e}(\boldsymbol{\sigma}^\star) \;:=\; \left\{ \sum_{K\in\mathcal{T}_h} \|\boldsymbol{\sigma}-\boldsymbol{\sigma}_h^\star\|^2_{\mathbf{div};K} \right\}^{1/2} ,$$

where $\widehat{\boldsymbol{\sigma}}_h$, p_h, $\mathbf{u}_h$, and $\boldsymbol{\sigma}_h^\star$ are computed according to (5.8), (5.12), (5.14), and (5.18), respectively. In turn, the associated experimental rates of convergence are given by

$$\mathtt{r}(\cdot) \;:=\; \frac{\log\big(\mathtt{e}(\cdot)\,/\,\mathtt{e}'(\cdot)\big)}{\log(h\,/\,h')} ,$$

where $\mathtt{e}$ and $\mathtt{e}'$ denote the corresponding errors for two consecutive meshes with sizes h and h', respectively. The numerical results presented below were obtained using a MATLAB code, where the corresponding linear systems were solved using its instruction "\" as main solver.

In Example 1 we consider $\Omega := (-0.5, 1.5)\times(0,2)$, $\mu = \alpha = 0.1$, and choose the data $\mathbf{f}$ and $\mathbf{g}$ so that the exact solution is given by the flow from [28], that is,

$$\mathbf{u}(\mathbf{x}) \;=\; \begin{pmatrix} 1-\exp(\lambda x_1)\cos(2\pi x_2) \\ \dfrac{\lambda}{2\pi}\exp(\lambda x_1)\sin(2\pi x_2) \end{pmatrix} \quad\text{and}\quad p(\mathbf{x}) \;=\; \frac{1}{2}\exp(2\lambda x_1) \;-\; \frac{1}{8\lambda}\big\{\exp(3\lambda)-\exp(-\lambda)\big\} ,$$

for all $\mathbf{x} := (x_1,x_2)^{\mathtt{t}} \in \Omega$, where $\lambda := \frac{Re}{2} - \sqrt{\frac{Re^2}{4}+4\pi^2}$ and $Re := \mu^{-1} = 10$ is the Reynolds number. Then, in Tables 6.1 up to 6.3 we summarize the convergence history of the mixed virtual element scheme (5.3) as applied to Example 1, using the $\mathbb{L}^2$-projection. We notice there that the rate of convergence of $O(h^{k+1})$ predicted by Theorems 5.4 and 5.5 (when $r = k+1$) is attained for all the unknowns of this smooth example, for triangular as well as for quadrilateral and hexagonal meshes. In particular, these results confirm that our postprocessed pseudostress $\boldsymbol{\sigma}_h^\star$ improves in one power the unsatisfactory order provided by the first approximation $\widehat{\boldsymbol{\sigma}}_h$ with respect to the broken $\mathbb{H}(\mathbf{div})$-norm. In turn, in Tables 6.4 up to 6.6 we present the convergence history of this example when using the $\mathbb{CG}$-projection instead. Note that basically the same results were obtained with this projection. On the other hand, in order to illustrate the accurateness of the discrete scheme, in Figures 6.1 and 6.2 we display some components of the approximate solutions for $k = 2$ and the second meshes of each decomposition, using only the $\mathbb{L}^2$-projection (no difference are observed with respect to the $\mathbb{CG}$-projection).

In Example 2 we follow [17], and consider the L-shaped domain $\Omega := (-1,1)^2 \setminus [0,1]^2$, $\mu = 1$, $\alpha = 0.5$, and choose the data $\mathbf{f}$ and $\mathbf{g}$ so that the exact solution is given by

$$\mathbf{u}(\mathbf{x}) \;=\; \begin{pmatrix} x_2^2 \\ -x_1^2 \end{pmatrix} \quad\text{and}\quad p(\mathbf{x}) \;=\; (x_1^2 \,+\, x_2^2)^{1/3} \,-\, p_0 ,$$

for all $\mathbf{x} := (x_1,x_2)^{\mathtt{t}} \in \Omega$, where $p_0 \in \mathrm{R}$ is such that $\int_\Omega p = 0$ holds. Note in this example that the partial derivatives of p, and hence, in particular $\mathbf{div}(\boldsymbol{\sigma})$, are singular at the origin. More precisely, because of the power 1/3, there holds $\boldsymbol{\sigma} \in \mathbb{H}^{5/3-\epsilon}(\Omega)$ and $\mathbf{div}(\boldsymbol{\sigma}) \in \mathbf{H}^{2/3-\epsilon}(\Omega)$ for each $\epsilon > 0$. Then, in Tables 6.7 up to 6.12 we display the corresponding convergence history of Example 2, using again the two projections introduced in Section 4.4. As predicted by the theory, and due to the limited regularity of p and $\boldsymbol{\sigma}$ in this case, we observe that the orders $O(h^{\min\{k+1,5/3\}})$ and $O(h^{2/3})$ are attained by $(\widehat{\boldsymbol{\sigma}}_h, p_h)$ and $\boldsymbol{\sigma}_h^\star$, respectively. In addition, we notice that $\mathbf{u}_h$ shows a convergence rate of $O(h^{\min\{k,5/3\}+1})$. This behaviour of the error $\|\mathbf{u}-\mathbf{u}_h\|_{0,\Omega}$ is explained by the fact that, as shown by (5.15), it depends on the regularity of $\mathbf{u}$, $\boldsymbol{\sigma}$, and $\mathbf{div}(\boldsymbol{\sigma})$. Finally, some components of the approximate solutions are displayed in Figures 6.3 and 6.4. Once again, we use $k = 2$, the second mesh of each decomposition and the $\mathbb{L}^2$-projection.

k	h	N	$\mathtt{e}(\boldsymbol{\sigma})$	$\mathtt{r}(\boldsymbol{\sigma})$	$\mathtt{e}(\mathbf{u})$	$\mathtt{r}(\mathbf{u})$	$\mathtt{e}(p)$	$\mathtt{r}(p)$	$\mathtt{e}(\boldsymbol{\sigma}^\star)$	$\mathtt{r}(\boldsymbol{\sigma}^\star)$
	0.2000	1241	1.53e-0	−−	6.24e-1	−−	8.51e-1	−−	5.28e-0	−−
	0.1000	4881	7.95e-1	0.94	2.61e-1	1.26	4.43e-1	0.94	2.74e-0	0.94
0	0.0500	19361	4.01e-1	0.99	1.22e-1	1.09	2.23e-1	0.99	1.38e-0	0.99
	0.0333	43441	2.68e-1	1.00	8.04e-2	1.03	1.49e-1	1.00	9.25e-1	1.00
	0.0250	77121	2.01e-1	1.00	6.00e-2	1.02	1.12e-1	1.00	6.94e-1	1.00
	0.2000	4881	1.54e-1	−−	6.03e-2	−−	9.93e-2	−−	6.02e-1	−−
	0.1000	19361	4.13e-2	1.90	1.49e-2	2.02	2.64e-2	1.91	1.59e-1	1.92
1	0.0500	77121	1.07e-2	1.95	3.69e-3	2.01	6.71e-3	1.98	4.04e-2	1.98
	0.0333	173281	4.83e-3	1.96	1.64e-3	2.00	2.99e-3	1.99	1.80e-2	1.99
	0.0250	307841	2.74e-3	1.97	9.22e-4	2.00	1.69e-3	1.99	1.01e-2	1.99
	0.2000	10121	1.53e-2	−−	5.32e-3	−−	9.74e-3	−−	5.14e-2	−−
	0.1000	40241	1.97e-3	2.96	6.52e-4	3.03	1.25e-3	2.96	6.82e-3	2.91
2	0.0500	160481	2.47e-4	2.99	8.11e-5	3.01	1.57e-4	2.99	8.65e-4	2.98
	0.0333	360721	7.31e-5	3.00	2.40e-5	3.00	4.65e-5	3.00	2.57e-4	2.99
	0.0250	640961	3.08e-5	3.00	1.01e-5	3.00	1.96e-5	3.00	1.09e-4	3.00

Table 6.1: Example 1, refinement with triangles and using the $\mathbb{L}^2$-projection.

k	h	N	$\mathtt{e}(\boldsymbol{\sigma})$	$\mathtt{r}(\boldsymbol{\sigma})$	$\mathtt{e}(\mathbf{u})$	$\mathtt{r}(\mathbf{u})$	$\mathtt{e}(p)$	$\mathtt{r}(p)$	$\mathtt{e}(\boldsymbol{\sigma}^\star)$	$\mathtt{r}(\boldsymbol{\sigma}^\star)$
	0.2336	1681	1.38e-0	−−	5.27e-1	−−	9.33e-1	−−	5.83e-0	−−
	0.1161	5625	7.18e-1	0.93	2.48e-1	1.08	4.91e-1	0.92	3.11e-0	0.90
0	0.0580	22201	3.34e-1	1.10	1.16e-1	1.10	2.29e-1	1.10	1.46e-0	1.09
	0.0387	49729	2.15e-1	1.09	7.59e-2	1.04	1.47e-1	1.09	9.39e-1	1.09
	0.0290	88209	1.58e-1	1.07	5.66e-2	1.02	1.08e-1	1.07	6.90e-1	1.07
	0.2336	5761	1.58e-1	−−	6.80e-2	−−	1.06e-1	−−	6.75e-1	−−
	0.1161	19463	4.35e-2	1.85	1.69e-2	1.99	2.96e-2	1.83	1.89e-1	1.82
1	0.0580	77257	9.49e-3	2.20	3.74e-3	2.18	6.46e-3	2.19	4.14e-2	2.19
	0.0387	173383	3.88e-3	2.21	1.59e-3	2.11	2.63e-3	2.21	1.69e-2	2.21
	0.0290	307841	2.07e-3	2.19	8.75e-4	2.08	1.40e-3	2.20	9.03e-3	2.19
	0.2336	11441	1.79e-2	−−	6.39e-3	−−	1.20e-2	−−	5.53e-2	−−
	0.1161	38777	2.28e-3	2.95	7.82e-4	3.00	1.55e-3	2.93	8.32e-3	2.71
2	0.0580	154217	2.21e-4	3.36	8.13e-5	3.26	1.50e-4	3.36	8.81e-4	3.24
	0.0387	346321	5.70e-5	3.35	2.25e-5	3.17	3.85e-5	3.36	2.32e-4	3.29
	0.0290	615089	2.18e-5	3.33	9.17e-6	3.12	1.47e-5	3.35	8.99e-5	3.29

Table 6.2: Example 1, refinement with quadrilaterals and using the $\mathbb{L}^2$-projection.

k	h	N	$\mathtt{e}(\boldsymbol{\sigma})$	$\mathtt{r}(\boldsymbol{\sigma})$	$\mathtt{e}(\mathbf{u})$	$\mathtt{r}(\mathbf{u})$	$\mathtt{e}(p)$	$\mathtt{r}(p)$	$\mathtt{e}(\boldsymbol{\sigma}^\star)$	$\mathtt{r}(\boldsymbol{\sigma}^\star)$
	0.0930	6003	6.72e-1	−−	2.66e-1	−−	4.56e-1	−−	2.92e-0	−−
	0.0738	10203	5.17e-1	1.13	2.00e-1	1.24	3.52e-1	1.12	2.25e-0	1.13
0	0.0556	18003	3.90e-1	1.00	1.53e-1	0.94	2.65e-1	1.00	1.70e-0	0.99
	0.0400	36003	2.75e-1	1.05	1.06e-1	1.11	1.87e-1	1.05	1.20e-0	1.05
	0.0294	66003	2.02e-1	1.01	7.78e-2	1.01	1.37e-1	1.01	8.82e-1	1.01
	0.0930	18005	3.71e-2	−−	1.85e-2	−−	2.45e-2	−−	1.60e-1	−−
	0.0738	30605	2.20e-2	2.28	1.06e-2	2.43	1.46e-2	2.25	9.44e-2	2.27
1	0.0556	54005	1.26e-2	1.95	6.18e-3	1.90	8.38e-3	1.96	5.46e-2	1.93
	0.0400	108005	6.27e-3	2.12	2.99e-3	2.19	4.17e-3	2.11	2.71e-2	2.11
	0.0294	198005	3.38e-3	2.01	1.62e-3	2.01	2.25e-3	2.01	1.47e-2	2.00
	0.0930	34007	1.95e-3	−−	9.04e-4	−−	1.25e-3	−−	6.24e-3	−−
	0.0738	57807	8.67e-4	3.51	3.88e-4	3.67	5.59e-4	3.50	2.81e-3	3.45
2	0.0556	102007	3.75e-4	2.96	1.78e-4	2.76	2.41e-4	2.97	1.26e-3	2.85
	0.0400	204007	1.26e-4	3.31	5.93e-5	3.32	8.06e-5	3.31	4.36e-4	3.19
	0.0294	374007	4.96e-5	3.03	2.35e-5	3.02	3.18e-5	3.03	1.74e-4	2.99

Table 6.3: Example 1, refinement with hexagons and using the $\mathbb{L}^2$-projection.

We end this paper by remarking that the numerical examples presented in this section confirm the suitability of our mixed virtual element scheme, based on either the $\mathbb{L}^2$ or the $\mathbb{CG}$ projection, to

k	h	N	$\mathtt{e}(\boldsymbol{\sigma})$	$\mathtt{r}(\boldsymbol{\sigma})$	$\mathtt{e}(\mathbf{u})$	$\mathtt{r}(\mathbf{u})$	$\mathtt{e}(p)$	$\mathtt{r}(p)$	$\mathtt{e}(\boldsymbol{\sigma}^\star)$	$\mathtt{r}(\boldsymbol{\sigma}^\star)$
	0.2000	1241	1.53e-0	−−	6.24e-1	−−	8.51e-1	−−	5.28e-0	−−
	0.1000	4881	7.95e-1	0.94	2.61e-1	1.26	4.43e-1	0.94	2.74e-0	0.94
0	0.0500	19361	4.01e-1	0.99	1.22e-1	1.09	2.23e-1	0.99	1.38e-0	0.99
	0.0333	43441	2.68e-1	1.00	8.04e-2	1.03	1.49e-1	1.00	9.25e-1	1.00
	0.0250	77121	2.01e-1	1.00	6.00e-2	1.02	1.12e-1	1.00	6.94e-1	1.00
	0.2000	4881	1.56e-1	−−	6.03e-2	−−	1.00e-1	−−	6.02e-1	−−
	0.1000	19361	4.17e-2	1.90	1.49e-2	2.02	2.66e-2	1.91	1.59e-1	1.92
1	0.0500	77121	1.08e-2	1.95	3.69e-3	2.01	6.75e-3	1.98	4.04e-2	1.98
	0.0333	173281	4.86e-3	1.97	1.64e-3	2.00	3.01e-3	1.99	1.80e-2	1.99
	0.0250	307841	2.76e-3	1.97	9.22e-4	2.00	1.69e-3	2.00	1.02e-2	1.99
	0.2000	10121	2.10e-2	−−	5.39e-3	−−	1.40e-2	−−	5.35e-2	−−
	0.1000	40241	2.76e-3	2.93	6.55e-4	3.04	1.85e-3	2.92	7.10e-3	2.91
2	0.0500	160481	3.51e-4	2.98	8.12e-5	3.01	2.35e-4	2.97	9.02e-4	2.98
	0.0333	360721	1.04e-4	2.99	2.40e-5	3.00	7.00e-5	2.99	2.68e-4	2.99
	0.0250	640961	4.42e-5	2.99	1.01e-5	3.00	2.96e-5	2.99	1.13e-4	3.00

Table 6.4: Example 1, refinement with triangles and using the $\mathbb{CG}$-projection.

k	h	N	$\mathtt{e}(\boldsymbol{\sigma})$	$\mathtt{r}(\boldsymbol{\sigma})$	$\mathtt{e}(\mathbf{u})$	$\mathtt{r}(\mathbf{u})$	$\mathtt{e}(p)$	$\mathtt{r}(p)$	$\mathtt{e}(\boldsymbol{\sigma}^\star)$	$\mathtt{r}(\boldsymbol{\sigma}^\star)$
	0.2336	1681	1.38e-0	−−	5.27e-1	−−	9.33e-1	−−	5.83e-0	−−
	0.1161	5625	7.18e-1	0.93	2.48e-1	1.08	4.91e-1	0.92	3.11e-0	0.90
0	0.0580	22201	3.34e-1	1.10	1.16e-1	1.10	2.29e-1	1.10	1.46e-0	1.09
	0.0387	49729	2.15e-1	1.09	7.59e-2	1.04	1.47e-1	1.09	9.39e-1	1.09
	0.0290	88209	1.58e-1	1.07	5.66e-2	1.02	1.08e-1	1.07	6.90e-1	1.07
	0.2336	5761	1.59e-1	−−	6.80e-2	−−	1.07e-1	−−	6.75e-1	−−
	0.1161	19463	4.36e-2	1.85	1.69e-2	1.99	2.96e-2	1.83	1.89e-1	1.82
1	0.0580	77257	9.49e-3	2.20	3.74e-3	2.18	6.46e-3	2.20	4.14e-2	2.19
	0.0387	173383	3.88e-3	2.21	1.59e-3	2.11	2.63e-3	2.22	1.69e-2	2.21
	0.0290	307841	2.07e-3	2.19	8.75e-4	2.08	1.40e-3	2.20	9.03e-3	2.19
	0.2336	11441	2.30e-2	−−	6.39e-3	−−	1.56e-2	−−	5.73e-2	−−
	0.1161	38777	3.42e-3	2.73	7.81e-4	3.01	2.36e-3	2.70	8.69e-3	2.70
2	0.0580	154217	3.59e-4	3.25	8.12e-5	3.26	2.50e-4	3.24	9.22e-4	3.23
	0.0387	346321	9.41e-5	3.30	2.25e-5	3.17	6.55e-5	3.30	2.43e-4	3.29
	0.0290	615089	3.64e-5	3.30	9.17e-6	3.12	2.53e-5	3.30	9.41e-5	3.29

Table 6.5: Example 1, refinement with quadrilaterals and using the $\mathbb{CG}$-projection.

k	h	N	$\mathtt{e}(\boldsymbol{\sigma})$	$\mathtt{r}(\boldsymbol{\sigma})$	$\mathtt{e}(\mathbf{u})$	$\mathtt{r}(\mathbf{u})$	$\mathtt{e}(p)$	$\mathtt{r}(p)$	$\mathtt{e}(\boldsymbol{\sigma}^\star)$	$\mathtt{r}(\boldsymbol{\sigma}^\star)$
	0.0930	6003	6.72e-1	−−	2.66e-1	−−	4.56e-1	−−	2.92e-0	−−
	0.0738	10203	5.17e-1	1.13	2.00e-1	1.24	3.52e-1	1.12	2.25e-0	1.13
0	0.0556	18003	3.90e-1	1.00	1.53e-1	0.94	2.65e-1	1.00	1.70e-0	0.99
	0.0400	36003	2.75e-1	1.05	1.06e-1	1.11	1.87e-1	1.05	1.20e-0	1.05
	0.0294	66003	2.02e-1	1.01	7.78e-2	1.01	1.37e-1	1.01	8.82e-1	1.01
	0.0930	18005	3.72e-2	−−	1.85e-2	−−	2.46e-2	−−	1.60e-1	−−
	0.0738	30605	2.20e-2	2.28	1.06e-2	2.43	1.46e-2	2.25	9.44e-2	2.27
1	0.0556	54005	1.27e-2	1.95	6.18e-3	1.90	8.39e-3	1.96	5.46e-2	1.93
	0.0400	108005	6.28e-3	2.12	2.99e-3	2.19	4.18e-3	2.11	2.72e-2	2.11
	0.0294	198005	3.39e-3	2.01	1.62e-3	2.01	2.25e-3	2.01	1.47e-2	2.00
	0.0930	34007	2.26e-3	−−	9.04e-4	−−	1.49e-3	−−	6.34e-3	−−
	0.0738	57807	1.02e-3	3.46	3.88e-4	3.67	6.75e-4	3.44	2.86e-3	3.45
2	0.0556	102007	4.27e-4	3.07	1.78e-4	2.76	2.81e-4	3.10	1.27e-3	2.87
	0.0400	204007	1.47e-4	3.22	5.93e-5	3.32	9.69e-5	3.22	4.42e-4	3.19
	0.0294	374007	5.71e-5	3.08	2.35e-5	3.02	3.75e-5	3.10	1.76e-4	3.00

Table 6.6: Example 1, refinement with hexagons and using the $\mathbb{CG}$-projection.

solve the Brinkman problem (2.1). Moreover, because of the rates of convergence obtained with the non-smooth Example 2, we realize that the approach will certainly be strengthened with the further

k	h	N	$\mathtt{e}(\boldsymbol{\sigma})$	$\mathtt{r}(\boldsymbol{\sigma})$	$\mathtt{e}(\mathbf{u})$	$\mathtt{r}(\mathbf{u})$	$\mathtt{e}(p)$	$\mathtt{r}(p)$	$\mathtt{e}(\boldsymbol{\sigma}^\star)$	$\mathtt{r}(\boldsymbol{\sigma}^\star)$
	0.1667	1345	1.70e-1	−−	7.89e-2	−−	5.47e-2	−−	1.95e-1	−−
	0.0833	5281	8.45e-2	1.01	3.93e-2	1.01	2.59e-2	1.08	1.10e-1	0.82
0	0.0435	19229	4.40e-2	1.00	2.05e-2	1.00	1.32e-2	1.03	6.62e-2	0.78
	0.0303	39469	3.06e-2	1.00	1.43e-2	1.00	9.19e-3	1.01	5.04e-2	0.75
	0.0217	76545	2.20e-2	1.00	1.02e-2	1.00	6.57e-3	1.01	3.94e-2	0.74
	0.1667	5281	2.86e-3	−−	2.20e-3	−−	1.78e-3	−−	4.47e-2	−−
	0.0833	20929	9.32e-4	1.62	5.49e-4	2.00	5.80e-4	1.62	2.82e-2	0.67
1	0.0435	76545	3.21e-4	1.64	1.49e-4	2.00	2.00e-4	1.64	1.82e-2	0.67
	0.0303	157345	1.77e-4	1.65	7.26e-5	2.00	1.10e-4	1.65	1.43e-2	0.67
	0.0217	305441	1.02e-4	1.65	3.74e-5	2.00	6.37e-5	1.65	1.15e-2	0.67
	0.1667	10945	4.95e-4	−−	1.52e-5	−−	3.30e-4	−−	2.57e-2	−−
	0.0833	43489	1.56e-4	1.67	2.40e-6	2.67	1.04e-4	1.67	1.62e-2	0.67
2	0.0435	159253	5.28e-5	1.67	4.23e-7	2.67	3.51e-5	1.67	1.05e-2	0.67
	0.0303	327493	2.89e-5	1.67	1.62e-7	2.67	1.93e-5	1.67	8.24e-3	0.67
	0.0217	635905	1.66e-5	1.67	6.67e-8	2.66	1.11e-5	1.67	6.61e-3	0.67

Table 6.7: Example 2, refinement with triangles and using the $\mathbb{L}^2$-projection.

k	h	N	$\mathtt{e}(\boldsymbol{\sigma})$	$\mathtt{r}(\boldsymbol{\sigma})$	$\mathtt{e}(\mathbf{u})$	$\mathtt{r}(\mathbf{u})$	$\mathtt{e}(p)$	$\mathtt{r}(p)$	$\mathtt{e}(\boldsymbol{\sigma}^\star)$	$\mathtt{r}(\boldsymbol{\sigma}^\star)$
	0.1667	1825	2.14e-1	−−	7.92e-2	−−	1.05e-1	−−	2.49e-1	−−
	0.0927	5985	8.75e-2	1.52	4.03e-2	1.15	3.59e-2	1.83	1.23e-1	1.20
0	0.0478	22533	3.83e-2	1.25	1.98e-2	1.08	1.24e-2	1.61	6.91e-2	0.87
	0.0321	49665	2.47e-2	1.10	1.31e-2	1.04	7.26e-3	1.34	5.13e-2	0.75
	0.0239	89441	1.81e-2	1.06	9.67e-3	1.03	5.07e-3	1.22	4.16e-2	0.72
	0.1667	6241	3.92e-3	−−	1.81e-3	−−	2.68e-3	−−	7.13e-2	−−
	0.0927	20681	1.20e-3	2.01	4.54e-4	2.36	8.32e-4	2.00	4.39e-2	0.83
1	0.0478	78347	3.66e-4	1.79	1.07e-4	2.17	2.54e-4	1.79	2.73e-2	0.72
	0.0321	173057	1.86e-4	1.71	4.70e-5	2.09	1.29e-4	1.70	2.08e-2	0.68
	0.0239	312009	1.13e-4	1.69	2.56e-5	2.06	7.88e-5	1.69	1.71e-2	0.67
	0.1667	12385	9.85e-4	−−	1.04e-5	−−	6.75e-4	−−	4.90e-2	−−
	0.0927	41185	3.13e-4	1.96	2.03e-6	2.78	2.14e-4	1.96	3.02e-2	0.83
2	0.0478	156349	9.68e-5	1.77	3.87e-7	2.50	6.61e-5	1.77	1.87e-2	0.72
	0.0321	345601	4.93e-5	1.70	1.41e-7	2.55	3.37e-5	1.70	1.43e-2	0.68
	0.0239	623329	3.00e-5	1.69	6.56e-8	2.59	2.05e-5	1.69	1.17e-2	0.67

Table 6.8: Example 2, refinement with quadrilaterals and using the $\mathbb{L}^2$-projection.

k	h	N	$\mathtt{e}(\boldsymbol{\sigma})$	$\mathtt{r}(\boldsymbol{\sigma})$	$\mathtt{e}(\mathbf{u})$	$\mathtt{r}(\mathbf{u})$	$\mathtt{e}(p)$	$\mathtt{r}(p)$	$\mathtt{e}(\boldsymbol{\sigma}^\star)$	$\mathtt{r}(\boldsymbol{\sigma}^\star)$
	0.0672	6933	7.86e-2	−−	4.09e-2	−−	2.29e-2	−−	1.17e-1	−−
	0.0385	19113	4.65e-2	0.94	2.46e-2	0.91	1.27e-2	1.06	8.04e-2	0.68
0	0.0275	37341	3.31e-2	1.01	1.76e-2	0.99	8.79e-3	1.08	6.34e-2	0.71
	0.0214	61617	2.57e-2	1.01	1.37e-2	0.99	6.76e-3	1.05	5.30e-2	0.71
	0.0170	97173	2.04e-2	1.00	1.09e-2	1.00	5.33e-3	1.03	4.51e-2	0.70
	0.0672	20795	1.15e-3	−−	5.24e-4	−−	7.91e-4	−−	4.65e-2	−−
	0.0385	57335	4.92e-4	1.52	1.89e-4	1.83	3.40e-4	1.52	3.29e-2	0.62
1	0.0275	112019	2.83e-4	1.64	9.67e-5	1.99	1.96e-4	1.64	2.64e-2	0.65
	0.0214	184847	1.86e-4	1.67	5.86e-5	1.99	1.29e-4	1.67	2.23e-2	0.68
	0.0170	291515	1.28e-4	1.64	3.70e-5	2.00	8.81e-5	1.64	1.91e-2	0.67
	0.0672	39277	3.67e-4	−−	1.71e-6	−−	2.55e-4	−−	3.23e-2	−−
	0.0385	108297	1.56e-4	1.54	4.54e-7	2.38	1.08e-4	1.54	2.28e-2	0.62
2	0.0275	211589	8.94e-5	1.65	1.82e-7	2.71	6.21e-5	1.65	1.84e-2	0.65
	0.0214	349153	5.85e-5	1.69	9.72e-8	2.51	4.06e-5	1.69	1.55e-2	0.68
	0.0170	550637	4.00e-5	1.65	5.11e-8	2.78	2.78e-5	1.64	1.33e-2	0.67

Table 6.9: Example 2, refinement with hexagons and using the $\mathbb{L}^2$-projection.

incorporation of an adaptive strategy based on a proper *a posteriori* error estimator. This issue will be addressed in a separate work.

k	h	N	$\mathtt{e}(\boldsymbol{\sigma})$	$\mathtt{r}(\boldsymbol{\sigma})$	$\mathtt{e}(\mathbf{u})$	$\mathtt{r}(\mathbf{u})$	$\mathtt{e}(p)$	$\mathtt{r}(p)$	$\mathtt{e}(\boldsymbol{\sigma}^\star)$	$\mathtt{r}(\boldsymbol{\sigma}^\star)$
	0.1667	1345	1.70e-1	−−	7.89e-2	−−	5.47e-2	−−	1.95e-1	−−
	0.0833	5281	8.45e-2	1.01	3.93e-2	1.01	2.59e-2	1.08	1.10e-1	0.82
0	0.0435	19229	4.40e-2	1.00	2.05e-2	1.00	1.32e-2	1.03	6.62e-2	0.78
	0.0303	39469	3.06e-2	1.00	1.43e-2	1.00	9.19e-3	1.01	5.04e-2	0.75
	0.0217	76545	2.20e-2	1.00	1.02e-2	1.00	6.57e-3	1.01	3.94e-2	0.74
	0.1667	5281	2.86e-3	−−	2.20e-3	−−	1.79e-3	−−	4.47e-2	−−
	0.0833	20929	9.29e-4	1.62	5.49e-4	2.00	5.81e-4	1.62	2.82e-2	0.67
1	0.0435	76545	3.20e-4	1.64	1.49e-4	2.00	2.00e-4	1.64	1.82e-2	0.67
	0.0303	157345	1.76e-4	1.65	7.26e-5	2.00	1.10e-4	1.65	1.43e-2	0.67
	0.0217	305441	1.02e-4	1.65	3.74e-5	2.00	6.37e-5	1.65	1.15e-2	0.67
	0.1667	10945	6.34e-4	−−	2.65e-5	−−	4.33e-4	−−	2.57e-2	−−
	0.0833	43489	2.00e-4	1.67	4.18e-6	2.67	1.36e-4	1.67	1.62e-2	0.67
2	0.0435	159253	6.75e-5	1.67	7.38e-7	2.67	4.61e-5	1.67	1.05e-2	0.67
	0.0303	327493	3.70e-5	1.67	2.82e-7	2.67	2.53e-5	1.67	8.24e-3	0.67
	0.0217	635905	2.13e-5	1.67	1.16e-7	2.67	1.45e-5	1.67	6.61e-3	0.67

Table 6.10: Example 2, refinement with triangles and using the $\mathbb{CG}$-projection.

k	h	N	$\mathtt{e}(\boldsymbol{\sigma})$	$\mathtt{r}(\boldsymbol{\sigma})$	$\mathtt{e}(\mathbf{u})$	$\mathtt{r}(\mathbf{u})$	$\mathtt{e}(p)$	$\mathtt{r}(p)$	$\mathtt{e}(\boldsymbol{\sigma}^\star)$	$\mathtt{r}(\boldsymbol{\sigma}^\star)$
	0.1667	1825	2.14e-1	−−	7.92e-2	−−	1.05e-1	−−	2.49e-1	−−
	0.0927	5985	8.75e-2	1.52	4.03e-2	1.15	3.59e-2	1.83	1.23e-1	1.20
0	0.0478	22533	3.83e-2	1.25	1.98e-2	1.08	1.24e-2	1.61	6.91e-2	0.87
	0.0321	49665	2.47e-2	1.10	1.31e-2	1.04	7.26e-3	1.34	5.13e-2	0.75
	0.0239	89441	1.81e-2	1.06	9.67e-3	1.03	5.07e-3	1.22	4.16e-2	0.72
	0.1667	6241	3.92e-3	−−	1.81e-3	−−	2.72e-3	−−	7.13e-2	−−
	0.0927	20681	1.21e-3	2.01	4.54e-4	2.36	8.43e-4	2.00	4.39e-2	0.83
1	0.0478	78347	3.67e-4	1.80	1.07e-4	2.17	2.57e-4	1.79	2.73e-2	0.72
	0.0321	173057	1.86e-4	1.71	4.70e-5	2.09	1.30e-4	1.71	2.08e-2	0.68
	0.0239	312009	1.13e-4	1.69	2.56e-5	2.06	7.93e-5	1.69	1.71e-2	0.67
	0.1667	12385	9.83e-4	−−	7.12e-6	−−	6.82e-4	−−	4.90e-2	−−
	0.0927	41185	3.18e-4	1.92	1.45e-6	2.72	2.21e-4	1.92	3.02e-2	0.83
2	0.0478	156349	1.01e-4	1.73	2.56e-7	2.61	7.03e-5	1.73	1.87e-2	0.72
	0.0321	345601	5.21e-5	1.67	9.08e-8	2.61	3.62e-5	1.68	1.43e-2	0.68
	0.0239	623329	3.19e-5	1.67	4.19e-8	2.63	2.21e-5	1.67	1.17e-2	0.67

Table 6.11: Example 2, refinement with quadrilaterals and using the $\mathbb{CG}$-projection.

k	h	N	$\mathtt{e}(\boldsymbol{\sigma})$	$\mathtt{r}(\boldsymbol{\sigma})$	$\mathtt{e}(\mathbf{u})$	$\mathtt{r}(\mathbf{u})$	$\mathtt{e}(p)$	$\mathtt{r}(p)$	$\mathtt{e}(\boldsymbol{\sigma}^\star)$	$\mathtt{r}(\boldsymbol{\sigma}^\star)$
	0.0672	6933	7.86e-2	−−	4.09e-2	−−	2.29e-2	−−	1.17e-1	−−
	0.0385	19113	4.65e-2	0.94	2.46e-2	0.91	1.27e-2	1.06	8.04e-2	0.68
0	0.0275	37341	3.31e-2	1.01	1.76e-2	0.99	8.79e-3	1.08	6.34e-2	0.71
	0.0214	61617	2.57e-2	1.01	1.37e-2	0.99	6.76e-3	1.05	5.30e-2	0.71
	0.0170	97173	2.04e-2	1.00	1.09e-2	1.00	5.33e-3	1.03	4.51e-2	0.70
	0.0672	20795	1.15e-3	−−	5.24e-4	−−	7.96e-4	−−	4.65e-2	−−
	0.0385	57335	4.95e-4	1.52	1.89e-4	1.83	3.42e-4	1.52	3.29e-2	0.62
1	0.0275	112019	2.85e-4	1.64	9.67e-5	1.99	1.97e-4	1.64	2.64e-2	0.65
	0.0214	184847	1.87e-4	1.67	5.86e-5	1.99	1.29e-4	1.67	2.23e-2	0.68
	0.0170	291515	1.28e-4	1.64	3.70e-5	2.00	8.87e-5	1.64	1.91e-2	0.67
	0.0672	39277	3.75e-4	−−	1.21e-6	−−	2.62e-4	−−	3.23e-2	−−
	0.0385	108297	1.59e-4	1.54	3.17e-7	2.41	1.11e-4	1.54	2.28e-2	0.62
2	0.0275	211589	9.13e-5	1.65	1.30e-7	2.65	6.38e-5	1.65	1.84e-2	0.65
	0.0214	349153	5.98e-5	1.69	6.84e-8	2.55	4.17e-5	1.69	1.55e-2	0.68
	0.0170	550637	4.09e-5	1.65	3.65e-8	2.73	2.85e-5	1.65	1.33e-2	0.67

Table 6.12: Example 2, refinement with hexagons and using the $\mathbb{CG}$-projection.

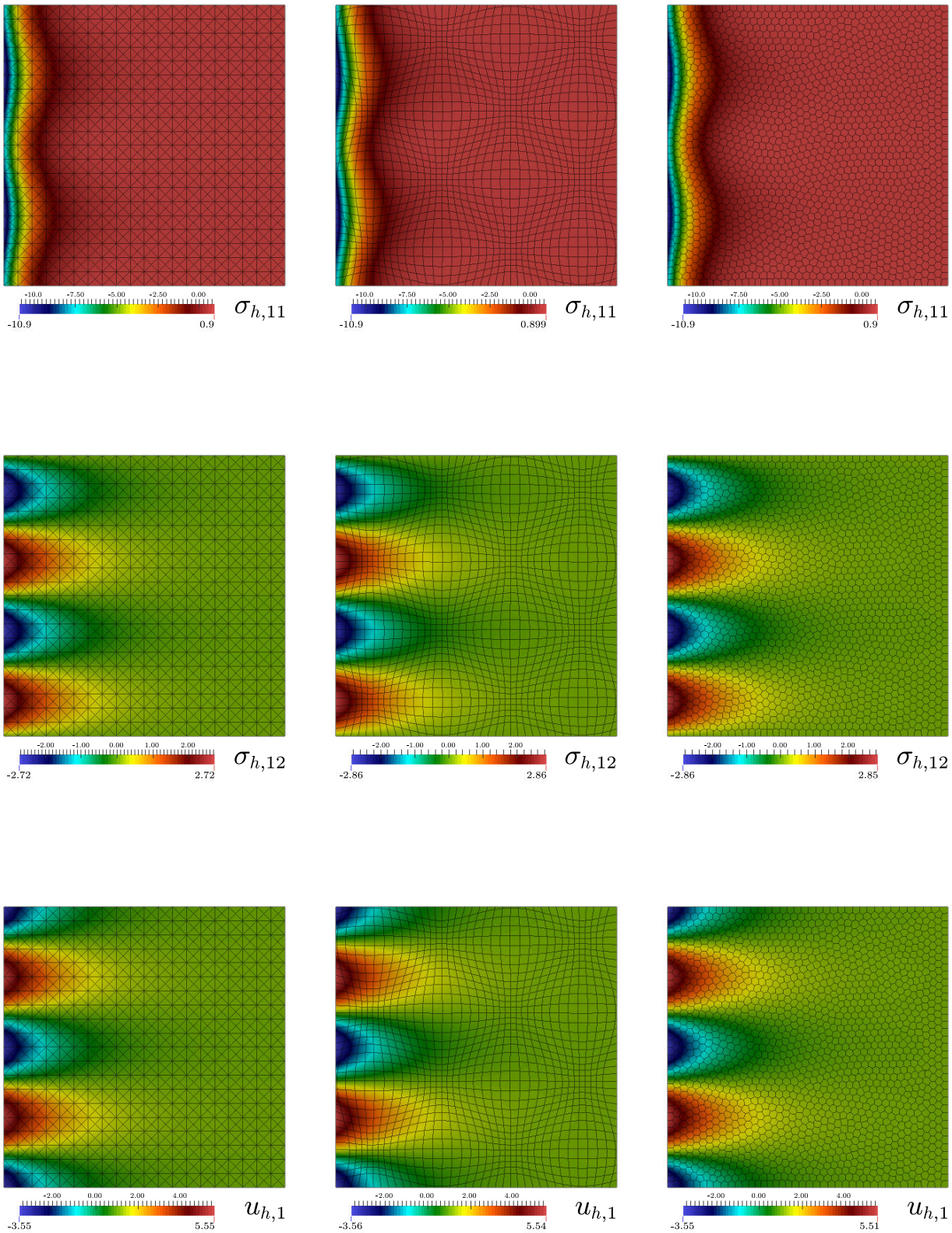

Figure 6.1: Example 1, $\sigma_{h,11}$ (top), $\sigma_{h,12}$ (center) and $u_{h,1}$ (bottom), using $k = 2$ and the second mesh of each kind (columns).

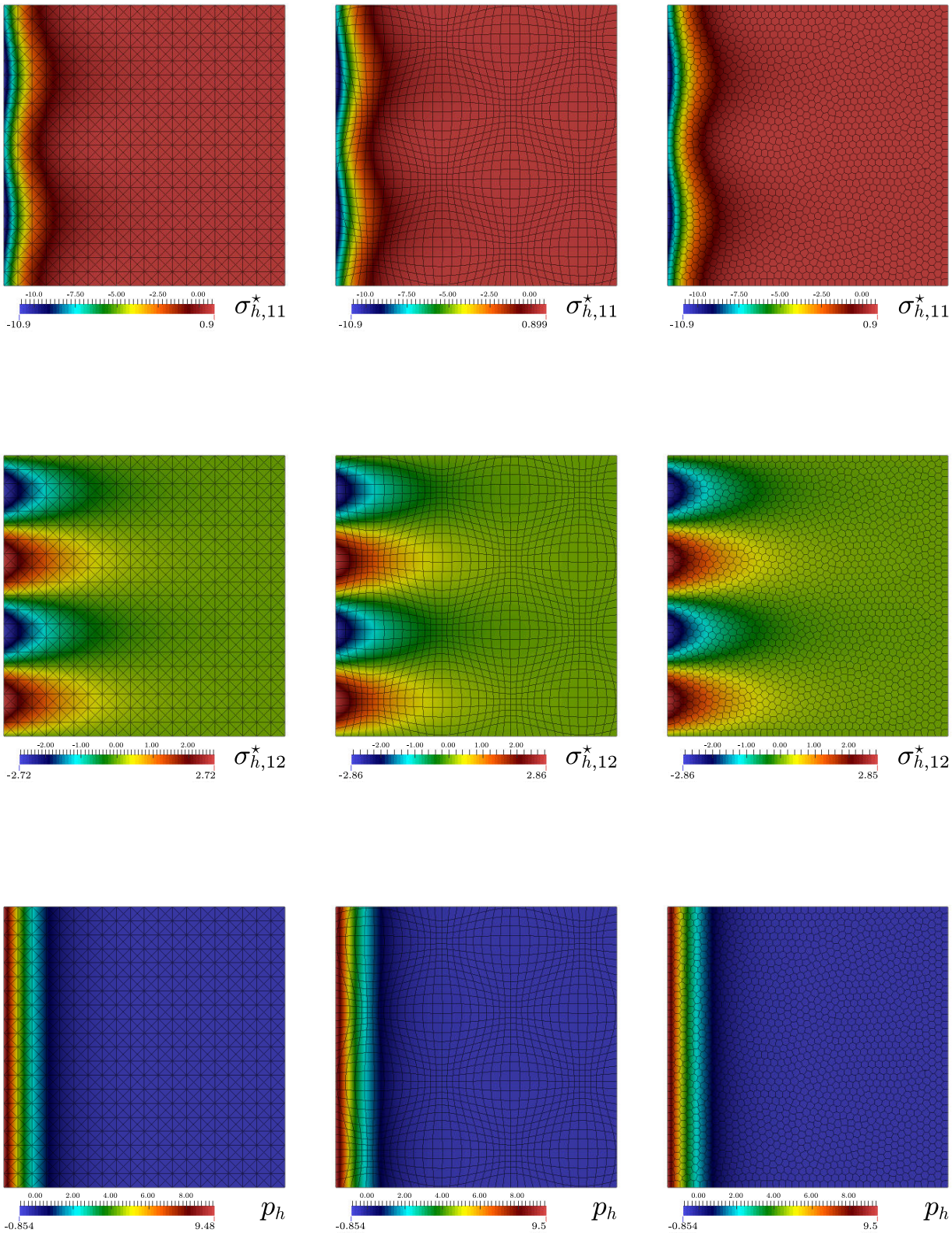

Figure 6.2: Example 1, $\sigma^\star_{h,11}$ (top), $\sigma^\star_{h,12}$ (center) and p_h (bottom), using $k = 2$ and the second mesh of each kind (columns).

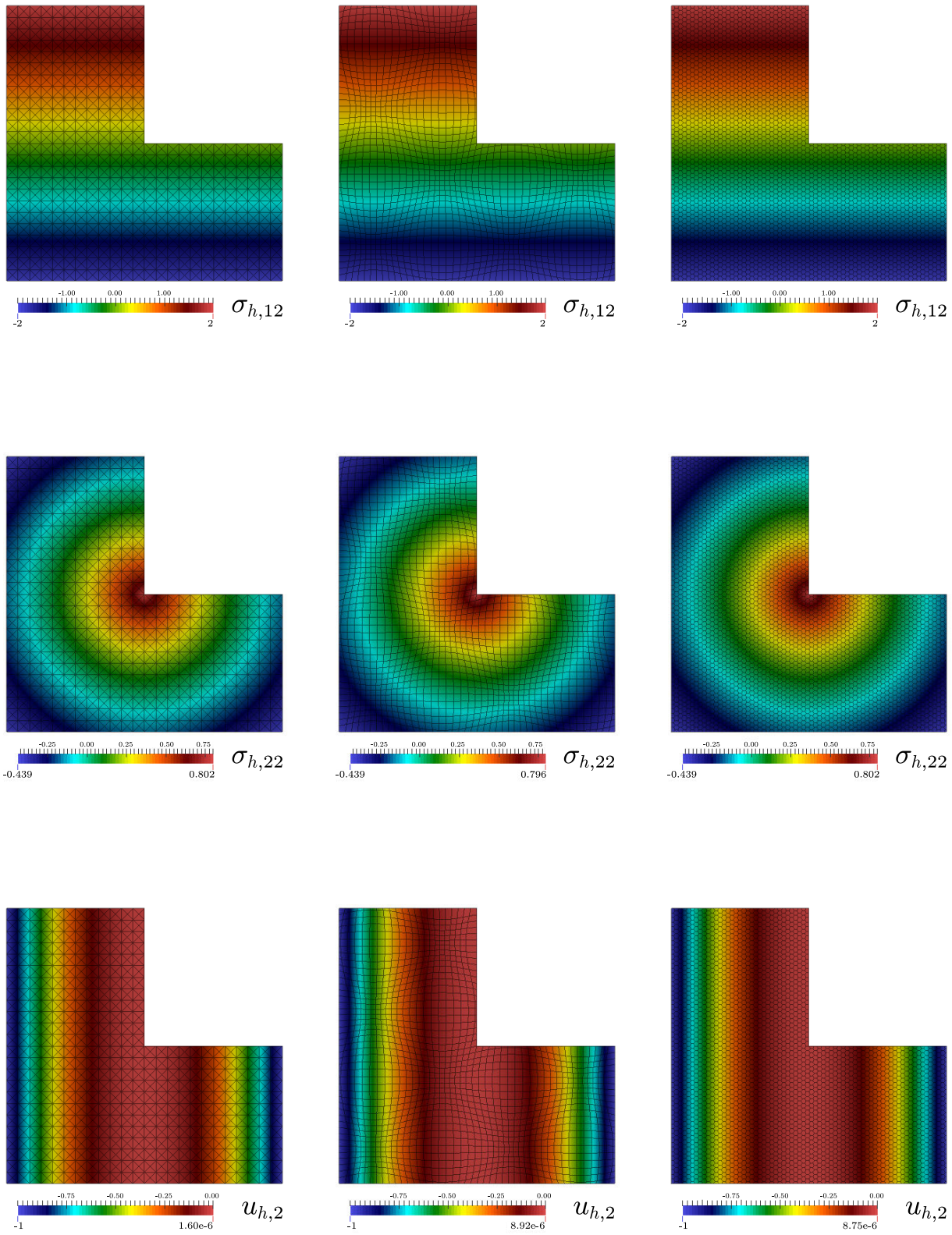

Figure 6.3: Example 2, $\sigma_{h,12}$ (top), $\sigma_{h,22}$ (center) and $u_{h,2}$ (bottom), using $k = 2$ and the second mesh of each kind (columns).

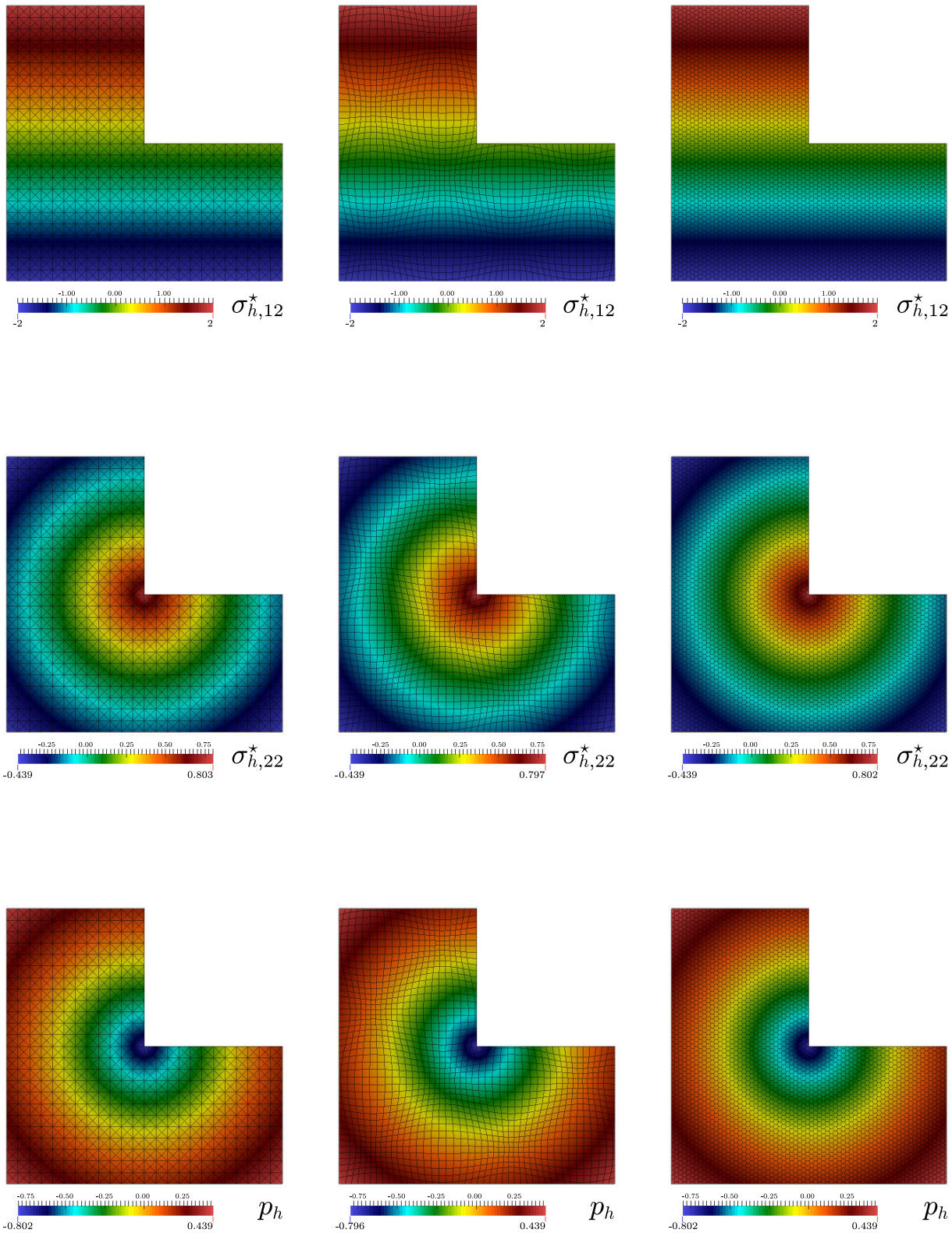

Figure 6.4: Example 2, $\sigma^\star_{h,12}$ (top), $\sigma^\star_{h,22}$ (center) and p_h (bottom), using $k = 2$ and the second mesh of each kind (columns).

References

[1] Ahmad, B., Alsaedi, A., Brezzi, F., Marini, L. D., and Russo, A. Equivalent projectors for virtual element methods. *Comput. Math. Appl. 66*, 3 (2013), 376–391.

[2] Anaya, V., Gatica, G. N., Mora, D., and Ruiz-Baier, R. An augmented velocity-vorticity-pressure formulation for the Brinkman equations. *Internat. J. Numer. Methods Fluids 79*, 3 (2015), 109–137.

[3] Anaya, V., Mora, D., Oyarzúa, R., and Ruiz-Baier, R. A priori and a posteriori error analysis of a mixed scheme for the Brinkman problem. *Numer. Math 133*, 4 (2016), 781–817.

[4] Anaya, V., Mora, D., Reales, C., and Ruiz-Baier, R. Stabilized mixed approximation of axisymmetric Brinkman flow. *ESAIM Math. Model. Numer. Anal. 49*, 3 (2015), 855–874.

[5] Antonietti, P. F., Beirão da Veiga, L., Mora, D., and Verani, M. A stream virtual element formulation of the Stokes problem on polygonal meshes. *SIAM J. Numer. Anal 52*, 1 (2014), 386–404.

[6] Beirão da Veiga, L., Brezzi, F., Cangiani, A., Marini, L. D., Manzini, G., and Russo, A. Basic principles of virtual elements methods. *Math. Models Methods Appl. Sci. 23*, 1 (2013), 199–214.

[7] Beirão da Veiga, L., Brezzi, F., and Marini, L. D. Virtual elements for linear elasticity problems. *SIAM J. Numer. Anal. 51*, 2 (2013), 794–812.

[8] Beirão da Veiga, L., Brezzi, F., Marini, L. D., and Russo, A. The hitchhiker's guide to the virtual element method. *Math. Models Methods Appl. Sci. 24*, 8 (2014), 1541–1573.

[9] Beirão da Veiga, L., Brezzi, F., Marini, L. D., and Russo, A. Mixed virtual element methods for general second order elliptic problems on polygonal meshes. *eprint arXiv:1506.07328v1* (2015).

[10] Beirão da Veiga, L., Brezzi, F., Marini, L. D., and Russo, A. $H(div)$ and $H(curl)$-conforming VEM. *Numer. Math. 133*, 2 (2016), 303–332.

[11] Beirão da Veiga, L., Brezzi, F., Marini, L. D., and Russo, A. Virtual element methods for general second-order elliptic problems on polygonal meshes. *Math. Models Methods Appl. Sci. 26*, 4 (2016), 729–750.

[12] Brezzi, F., Cangiani, A., Manzini, G., and Russo, A. Mimetic finite differences and virtual element methods for diffusion problems on polygonal meshes. *I.M.A.T.I.-C.N.R., Technical Report 22PV12/0/0* (2012), 1–27.

[13] Brezzi, F., Falk, R. S., and Marini, L. D. Basic principles of mixed virtual element methods. *ESAIM Math. Model. Numer. Anal. 48*, 4 (2014), 1227–1240.

[14] Brezzi, F., and Fortin, M. *Mixed and Hybrid Finite Element Methods*. Springer Verlag, 1991.

[15] Brezzi, F., and Marini, L. D. Virtual element methods for plate bending problems. *Comput. Methods Appl. Mech. Engrg. 253* (2013), 455–462.

[16] Cáceres, E. Mixed Virtual Element Methods. Applications in Fluid Mechanics. *Thesis leading to the professional title of Mathematical Civil Engineer, Universidad de Concepción, Chile* (2015).

[17] Cáceres, E., and Gatica, G. N. A mixed virtual element method for the pseudostress-velocity formulation of the Stokes problem. *IMA J. Numer. Anal. doi:10.1093/imanum/drw00* (2016).

[18] Figueroa, L., Gatica, G. N., and Márquez, A. Augmented mixed finite element methods for the stationary Stokes equations. *SIAM J. Sci. Comput. 31*, 2 (2008/09), 1082–1119.

[19] Gain, A. L., Talischi, C., and Paulino, G. H. On the virtual element method for three-dimensional linear elasticity problems on arbitrary polyhedral meshes. *Comput. Methods Appl. Mech. Engrg 282* (2014), 132–160.

[20] Gatica, G. N., Gatica, L. F., and Márquez, A. Analysis of a pseudostress-based mixed finite element method for the Brinkman model of porous media flow. *Numer. Math. 126*, 4 (2014), 635–677.

[21] Gatica, G. N., Gatica, L. F., and Sequeira, F. A. Analysis of an augmented pseudostress-based mixed formulation for a nonlinear Brinkman model of porous media flow. *Comput. Methods Appl. Mech. Engrg. 289*, 1 (2015), 104–130.

[22] Gatica, G. N., Gatica, L. F., and Sequeira, F. A. A $\mathbb{RT}_k - \mathbf{P}_k$ approximation for linear elasticity yielding a broken $\mathbb{H}(\mathbf{div})$ convergent postprocessed stress. *Appl. Math. Lett 49* (2015), 133–140.

[23] Gatica, G. N., Gatica, L. F., and Sequeira, F. A. A priori and a posteriori error analyses of a pseudostress-based mixed formulation for linear elasticity. *Comput. Math. Appl. 71*, 2 (2016), 585–614.

[24] Guzmán, J., and Neilan, M. A family of nonconforming elements for the Brinkman problem. *IMA J. Numer. Anal. 32*, 4 (2012), 1484–1508.

[25] Juntunen, M., and Stenberg, R. Analysis of finite element methods for the Brinkman problem. *Calcolo 47*, 3 (2010), 129–147.

[26] Könnö, J., and Stenberg, R. H(div)-conforming finite elements for the Brinkman problem. *Math. Models Methods Appl. Sci. 21*, 11 (2011), 2227–2248.

[27] Könnö, J., and Stenberg, R. Numerical computations with H(div)-finite elements for the Brinkman problem. *Comput. Geosci. 16*, 1 (2012), 139–158.

[28] Kovasznay, L. I. G. Laminar flow behind a two-dimensional grid. *Proc. Camb. Philos. Soc. 44* (1948), 58–62.

[29] Mora, D., Rivera, G., and Rodríguez, R. A virtual element method for the Steklov eigenvalue problem. *Math. Models Methods Appl. Sci. 25*, 8 (2015), 1421–1445.

[30] Talischi, C., Paulino, G. H., Pereira, A., and Menezes, I. F. PolyMesher: a general-purpose mesh generator for polygonal elements written in Matlab. *Struct. Multidisc. Optim. 45*, 3 (2012), 309–328.

[31] Vassilevski, P., and Villa, U. A mixed formulation for the Brinkman problem. *SIAM J. Numer. Anal 52*, 1 (2014), 258–281.